

Encoding of social signals in all three electrosensory pathways of *Eigenmannia virescens*

Anna Stöckl^{1,2}, Fabian Sinz^{3,4}, Jan Benda^{3,1} & Jan Grawe^{3,1,*}

¹*Department Biology II, Ludwig-Maximilians-Universität München, Germany*

²*Department of Biology, Lund University, Lund, Sweden*

³*Institut für Neurobiologie, Eberhardt Karls Universität Tübingen, Germany*

⁴*Bernstein Center for Computational Neuroscience, Tübingen, Germany*

*corresponding author: jan.grawe@uni-tuebingen.de

Abstract

Extracting complementary features in parallel pathways is a widely used strategy for a robust representation of sensory signals. Weakly electric fish offer the rare opportunity to study complementary encoding of social signals in all of its electrosensory pathways. Electrosensory information is conveyed in three parallel pathways: two receptor types of the tuberous (active) system and one receptor type of the ampullary (passive) system. Modulations of the fish's own electric field are sensed by these receptors and used in navigation, prey-detection and communication.

We studied the neuronal representation of electric communication signals (called chirps) in the ampullary and the two tuberous pathways of *Eigenmannia virescens*. We first characterized different kinds of chirps observed in behavioral experiments. Since *Eigenmannia* chirps simultaneously drive all three types of receptors, we studied their responses in *in vivo* electrophysiological recordings. Our results demonstrate that different electroreceptor types encode different aspects of the stimuli and each appears best suited to convey information about a certain chirp type. A decoding analysis of single neurons and small populations shows that this specialization leads to a complementary representation of information in the tuberous and ampullary receptors. This suggests that a potential readout mechanism

should combine information provided by the parallel processing streams to improve chirp detectability.

1 Introduction

Parallel processing of sensory information is a widely used strategy in nervous systems. Parallel channels can result either directly from different types of receptor neurons transducing distinct stimulus features or from neurons further downstream that process a common stimulus in distinct ways. A well known example for the latter is the mammalian visual system where different neuronal circuits extract color and motion information of a visual stimulus from the same receptors (Wässle, 2004; Nassi and Callaway, 2009). In other sensory modalities, like somatosensation, parallel processing already starts at the receptor level where different types of receptors extract separate aspects of the sensory input (Bensmaia, 2008).

Electroreception in wave-type weakly electric fish is another example for an early separation. Information about the electric field in the fish's vicinity is split into three pathways at the receptor level: The ampullary receptors of the passive electrosensory system detect low-frequency modulations of electric fields, like those created by muscle activity of other animals (Hopkins, 1976). T-units and P-units of the tuberous electrosensory system, on the other hand, are tuned to the high-frequencies of the electric organ discharge (EOD) generated by weakly electric fish itself. T-units encode the phase of EOD and consequently carry precise timing information (Scheich et al., 1973; Hopkins, 1976), while P-units spike with a probability that is proportional to the amplitude of the EOD which itself is modulated by nearby objects, prey, predators, as well as the fields of conspecifics (Bullock and Chichibu, 1965; Scheich et al., 1973; Hopkins, 1976; Zakon, 1986).

Weakly electric fish offer the unique opportunity to experimentally control and electrophysiologically assess the encoding and processing of social signals in the entire electrosensory system. Communication signals (chirps) of *E. virescens*, unlike those of other species of weakly electric fish, contain both low- and high-frequency components that drive all three electroceptrors (Hagedorn and Heiligenberg, 1985; Metzner and Heiligenberg, 1991; Hupé et al., 2008). Studying the neural representation of chirps on the receptor level is therefore important to es-

tablish the basis for further studies on electrocommunication in higher brain areas.

The main chirp type described in *E. virescens* are interruptions of the regular EOD which can last up to 2 s (Hopkins, 1974a; Hagedorn and Heiligenberg, 1985). During these interruptions the otherwise balanced EOD develops a DC-offset that gives rise to a low-frequency component stimulating the ampullary receptors (Hopkins, 1974a; Metzner and Heiligenberg, 1991). Interruptions accompany courtship and mating, are necessary to induce spawning in females (Hagedorn and Heiligenberg, 1985), but are also used in aggressive situations by both sexes (Hopkins, 1974a). In encounters with conspecifics amplitude modulations (AM) arise from the interference of the individual EODs. The EOD of each animal will be modulated with a frequency equal to the difference of the individual frequencies. The resulting AM is a beat that constitutes a background signal on which communication signals occur (e.g. Walz et al., 2014). In species in which the EOD frequency exhibits a sexualok dimorphism, the nature of the back-ground beat carries information about the type of social encounter (e.g. *Apteronotus* same-sex vs. different-sex encounter, see for example Hupé et al., 2008). In the South-American glass knifefish *Eigenmannia virescens* (Sternopygidae, Gymnotiformes) studied here, beats of low frequencies are actively avoided by a change of EOD frequencies in both individuals shifting the beat frequency out of the frequency range used for object detection and navigation. This so called jamming avoidance response (JAR) exemplifies how the information of two parallel sen-sory channels, T-units and P-units of the tuberous system are used to unambiguously determine the difference in EOD frequency and guide the behavior (Heiligenberg, 1991).

Chirp encoding in P-units of *Apteronotus leptorhynchus*, a species in which chirps exclusively affect the tuberous system, has been extensively studied in different social encounters, i.e. in different underlying beats (Benda et al., 2005, 2006; Hupé et al., 2008; Marsat and Maler, 2010; Vonderschen and Chacron, 2011; Walz et al., 2014). In *Eigenmannia*, however, the en-coding of EOD interruptions has previously only been assessed in the absence of an EOD of a second fish (Metzner and Heiligenberg, 1991). This means that the fish was stimulated solely with its own field and chirps whithout the beat pattern characteristic of social encounters. Here we investigated the encoding of different communication signals in the presence of a second fish producing chirps. We recorded the neuronal responses in all three types of electroreceptors. We set out by charaterizing electrical communication in behavioral experiments. We identify

an electric signal that has previously been anecdotally reported as an incomplete interruption, establish it as a chirp in its own right, and describe it in detail. Subsequent *in vivo* electrophysiological experiments show that this and previously described chirp types elicit qualitatively different responses in P- and T-units while the ampullary receptors encodes mainly the occurrence and duration of any type of chirp. In a decoding analysis of single neurons and small populations we demonstrate that the two systems provide complementary information about the different chirp types which can improve the detectability of these communication signals when combined.

2 Methods

All experimental protocols complied with national and European law and were approved by the Ethics Committee of the Ludwig-Maximilians Universität München (permit no: 55.2-1-54-2531-135-09). Individuals of *Eigenmannia virescens* were purchased from commercial fish dealers (Aquarium Glaser, Rodgau, Germany) and kept in colonies of up to 20 fish.

2.1 Behavioral experiments

Fourteen adult fish, 10 to 21 cm body length, were used for the behavioral experiments. Individual electric organ discharge (EOD) frequencies were between 220 and 550 Hz (383 ± 77 Hz s.d., temperature corrected to 26°C). Temperature correction was done applying the average Q10 estimated in seven animals ($Q10 = 1.41 \pm 0.11$ s.d.). We did not observe distinct clustering of EOD frequencies, which could have indicated a segregation between males and females, as has been observed in other species of weakly electric fish, such as *Apteronotus* (Zakon and Dunlap, 1999, e.g.) or *Sternopygus* (Zakon et al., 1991, e.g.). Following a phenomenological classification of sexual maturity as used by other authors (e.g. Kramer, 1987), all animals were sexually immature, since none of them were gravid with eggs (females, assessed by visual inspection) or in the range of 30 cm body length (males).

Behavioral experiments were conducted in a chirp chamber (Dye, 1987; Bastian et al., 2001; Engler and Zupanc, 2001; Dunlap and Oliveri, 2002) at water temperatures between 24 to 27°C. A fish was placed in a tube covered with a mesh in the middle of a 45 l tank. Via silver electrodes at the head and the tail the electric field was recorded. A pair of carbon rod electrodes, oriented parallel to the longitudinal axis of the fish, was used for stimulation. The fish was stimulated with sine waves of different frequencies mimicking a conspecific. Stimulus output strength was adjusted to approximately half the fish's EOD amplitude (in the range of 0.5 to 1.5 mV/cm). Difference frequencies (relative to the recorded EOD) of 100, 48, 24, 12, 4 and 0 Hz, both positive and negative, were used.

The head-to-tail-EOD signal was recorded using an extracellular amplifier (EXT 10-2F, npi-electronics, Tamm, Germany). Signals were amplified by a factor of 1000, and band-pass filtered with cutoff frequencies of 0.1 Hz and 30 kHz for the high- and low-pass filter, respectively.

Signals were sampled at 30 kHz using a National Instruments data acquisition card (PCI-6295, National Instruments, Austin TX, USA). Data was analyzed using Matlab (The Mathworks, Natick, MA). Stimulation and recording were controlled by the JAR plugin of the RELACS software package (www.relacs.net). Chirps were detected offline by selecting those frequency excursions that deviated more than 30 Hz from the baseline EOD frequency (see figure 1).

2.2 Electrophysiology

Surgery 22 *E. virescens* (10 to 21 cm) were used for single-unit recordings. Recordings of electroreceptors were made from the anterior part of the lateral line nerve.

Fish were initially anaesthetized with 150 mg/l MS-222 (PharmaQ, Fordingbridge, UK) until gill movements ceased and were then respirated with a constant flow of water through a mouth tube, containing 120 mg/l MS-222 during the surgery to sustain anaesthesia. The lateral line nerve was exposed dorsal to the operculum. Fish were fixed in the setup with a plastic rod glued to the exposed skull bone. The wounds were locally anaesthetized with Lidocaine-hydrochloride 2% (bela-pharm GmbH, Vechta, Germany) before exposing the nerve. Local anaesthesia was renewed every two hours by careful application of Lidocaine to the skin surrounding the wound.

After surgery, fish were immobilized with 0.05 ml 5 mg/ml tubocurarine (Sigma - Aldrich, Steinheim, Germany) injected into the trunk muscles. Since tubocurarine suppresses all muscular activity, it also suppresses the activity of the electrocytes of the electric organ and thus strongly reduces the EOD of the fish. We therefore mimicked the EOD by a sinusoidal signal provided by a sine-wave generator (Hameg HMF 2525, Hameg Instruments, Mainhausen, Germany) via silver electrodes in the mouth tube and at the tail. Amplitude and frequency of the artificial field were adjusted to the fish's own field as measured prior to surgery. After surgery, fish were transferred into the recording tank of the setup filled with water from the fish's housing tank not containing MS-222. Respiration was continued without anaesthesia. The animals were submerged into the water so that the exposed nerve was just above the water surface. Electroreceptors located on the parts above water surface did not respond to the stimulus and were excluded from analysis. Water temperature was kept at 26 °C.

Recording Action potentials from electroreceptor afferents were recorded intracellularly with sharp borosilicate microelectrodes (GB150F-8P, Science Products, Hofheim, Germany), pulled to a resistance between 20 and 100 M Ω and filled with a 1 M KCl solution. Electrodes were positioned by microdrives (Luigs-Neumann; Ratingen, Germany). As a reference, glass microelectrodes were used. They were placed in the tissue surrounding the nerve, adjusted to the isopotential line of the recording electrode. The potential between the micropipette and the reference electrode was amplified (SEC-05X, npi electronic GmbH; Tamm, Germany) and low-pass filtered at 10 kHz. Signals were digitized by a data acquisition board (PCI-6229, National Instruments, Austin TX, USA) at a sampling rate of 20 kHz. Spikes were detected and identified online based on the peak-detection algorithm proposed by Todd and Andrews (1999).

The EOD of the fish was measured between the head and tail via two carbon rod electrodes (11 cm long, 8 mm diameter). The potential at the skin of the fish was recorded by a pair of silver wires, spaced 1 cm apart, which were placed orthogonal to the side of the fish at two thirds body length. The residual EOD potentials were recorded and monitored with a pair of silver wire electrodes placed in a piece of tube that was put over the tip of the tail. These EOD voltages were amplified by a factor of 1000 and bandpass filtered between 3 Hz and 1.5 kHz (DPA-2FXM, npi-electronics, Tamm, Germany).

Stimuli were attenuated (ATN-01M, npi-electronics, Tamm, Germany), isolated from ground (ISO-02V, npi-electronics, Tamm, Germany), and delivered by two carbon rod electrodes (30 cm length, 8 mm diameter) placed on either side of the fish parallel to its longitudinal axis. Stimuli were calibrated to evoke defined amplitude modulations measured close to the fish. Spike and EOD detection, stimulus generation and attenuation, as well as pre-analysis of the data were performed online during the experiment within the RELACS software version 0.9.7 using the efish plugin-set (J.B., www.relacs.net).

Stimulation Chirp stimuli consisted DC playbacks of computer generated EOD traces containing simplified versions of the different types of EOD interruptions (figure 2). Stimuli mimicked conspecific fish with EOD frequencies 24 or 100 Hz above or below the receiving fish. We did not use smaller difference frequencies, since the two-sided jamming avoidance response of *E. virescens* resulted in difference frequencies of at least 20 Hz, which was in conformity with

observations in their natural habitat (Tan et al., 2005). The stimulus intensity was adjusted to amplitude modulations of 20 % contrast (relative to the amplitude of the fish field). The chirp types presented were single-cycle interruptions, multiple repetitions of single-cycle interruptions of 6 and 18 cycles length (termed type B chirps), as well as prolonged interruptions of 4 and 20 cycles length (type A chirps).

Every repetition of the stimulus contained 16 chirps, separated by 200 cycles of baseline EOD frequency and was presented between 15 and 25 times.

Data Analysis We computed continuous firing rates from spike trains by convolution with a Gaussian kernel of a standard deviation of 1 ms. Peri-stimulus-time-histograms (PSTH) were obtained by averaging continuous firing rates across trials.

The encoding of chirps was assessed by comparing various response features: the mean firing frequency, the response correlation across trials, and the first derivative of the PSTH.

These features were estimated in three different response sections (see also figure 3): (i) the *chirp response* was estimated in a window of a width that corresponded to the chirp duration plus an additional 2 ms in P-units, and 7 ms in ampullary receptors. In P- and T-units this window was shifted 3 ms relative to chirp onset to account for neuronal delays. In ampullary receptors the shift amounted to 5 ms. (ii) The *beat response* was calculated by using the same window and the same beat phase as before but in a beat containing no chirp. (iii) Measures derived from these two windows were compared to the *control response* which was calculated from a complete uninterrupted beat cycle for slow beats or several beat cycles at high beat frequencies in P- and T-units. For ampullary receptors the *control response* was calculated in an 80 ms window preceding chirp onset. Onset responses to chirps in P- and T-units were calculated similarly, but the length of the analysis windows for the *chirp response* and *beat response* were shortened to one EOD cycle.

The phase relation between the chirps and the beat was extracted during offline analysis. The phase of chirp onset (ϕ) was calculated as

$$\phi = 2\pi \frac{t_S - t_{EOD}}{T_{EOD}} \quad (1)$$

where t_{EOD} was the time of the last EOD cycle before chirp onset, t_S was the time of chirp onset and T_{EOD} the period of the EOD. We discriminated ten chirp phases, sorted the responses

of P-and T-units according to their onset phase and analysed them separately. Ten chirp phases provided fine enough binning to ensure that only chirps occurring in very similar phases would be analysed together, thus minimizing the effect of averaging out response characteristics across phases. Ampullary responses were pooled across phases since ampullary receptors are not driven by the beat.

We computed the mean firing rate in P-units and ampullary receptors. The mean spike train correlation and absolute derivative of the PSTH were only estimated in P-units. The mean firing rate was quantified as the average of the continuous spike train in the respective window and averaged over trials. The spike train correlation was quantified according to Benda et al. (2006) as the correlation coefficient

$$r_{ij} = \frac{\langle (s_i - \langle s_i \rangle_t)(s_j - \langle s_j \rangle_t) \rangle_t}{\sqrt{\langle (s_j - \langle s_j \rangle_t)^2 \rangle_t} \sqrt{\langle (s_j - \langle s_j \rangle_t)^2 \rangle_t}} \quad (2)$$

of all possible pairs, s_i and s_j , of spike trains evoked by repeated stimulation and convolved with a Gaussian. Brackets $\langle \cdot \rangle_t$ denote averages over time. The mean spike train correlation was obtained by averaging r_{ij} over all pairs of spike trains.

In T-units, the inter-spike intervals (ISIs) were used for the analysis of chirp responses. A continuous representation of ISIs was obtained by convolving ISIs with a Gaussian kernel with a standard deviation of 1 ms. Mean ISI and correlation of ISIs were computed as discussed for the firing rate of P-units.

Response duration in ampullary receptors was calculated as the time the firing rate exceeded baseline firing rate plus four times the standard deviation of the average baseline firing rate. This was adjusted by visual inspection to give the closest match with the chirp duration.

Decoding Analysis All decoding analyses were based on the numpy, sklearn, and matplotlib packages of python (Jones et al., 2001; Pedregosa et al., 2011; Hunter, 2007).

For the decoding analysis we extracted segments from the neuronal responses that either contained a chirp (chirp responses) or that were randomly placed in the inter-chirp interval, i.e. when the simulated second fish was present but did not chirp (baseline responses). The decoding task was to discriminate a chirp- from baseline responses. Our analysis was performed for the 24Hz beat condition. Since the EOD frequencies of the recorded fish varied between 280Hz

and 510Hz, the applied chirp stimuli had to vary accordingly. The width of the data segment was hence based on EOD cycles instead of fixed temporal durations. Data segments of duration $D \in 5, 10, 20, 25, 30$ EOD cycles were used.

We simulated small populations of receptor neurons by combining responses of different neurons recorded in the same animal to the same chirp type. Therefore, the number of trials for one particular chirp type was equal to the minimal number of trials for that condition for all neurons participating in the population. If more responses were recorded from one neuron, a random selection was dropped.

Support vector machines were used (SVMs; Boser et al., 1992; Cortes and Vapnik, 1995) to classify the receptor responses to a particular chirp type against its baseline activity. SVMs learn decision rules of the form

$$\hat{y} = \text{sign} \left(\sum_{i=1}^m \alpha_i k(x_i, x) + b \right) \quad (3)$$

from labeled data sets $\{(y_i, x_i)\}_{i=1}^m$, where $y_i \in \{-1, 1\}$ is the label that indicates whether a trial x_i is a chirp- or a baseline response. \hat{y} is the label that the SVM predicts for the trial x . The function k is a positive semi-definite Mercer kernel which corresponds to a dot-product $k(x, x_i) = \langle \phi(x), \phi(x_i) \rangle$ between two feature vectors $\phi(x)$ and $\phi(x_i)$ computed from the data points x and x_i , respectively (Schölkopf and Smola, 2002). Using the bi-linearity of the dot-product, one can see that the inner part of equation (3) is a linear function of the feature vector $\phi(x)$

$$\sum_{i=1}^m \alpha_i k(x_i, x) + b = \left\langle \sum_{i=1}^m \alpha_i \phi(x_i), \phi(x) \right\rangle + b = \langle w, \phi(x) \rangle + b \text{ for } w = \sum_{i=1}^m \alpha_i \phi(x_i). \quad (4)$$

In all analyses for single neurons, we use

$$k(x_1, x_2) = \int_0^T (x_1 * h)(t) (x_2 * h)(t) dt, \quad (5)$$

where $x_\ell * h$ denotes the convolution of a filter kernel h with a spike train $x_\ell = \sum_i \delta(t - t_i^{(\ell)})$. We use a one-sided exponential filter $h(t) = [t]_+ \cdot \exp(-\frac{t}{\tau})$ with $\tau = 1$ ms in order to simulate the input to a pyramidal cell post-synaptic to the receptors. Equation (5) can be computed more efficiently by solving the integral analytically resulting in (Park et al., 2013)

$$k(x_1, x_2) = \int_0^T (x_1 * h)(t) (x_2 * h)(t) dt = \frac{\tau}{2} \sum_{i,j} \exp \left(-\frac{|t_i^{(1)} - t_j^{(2)}|}{\tau} \right),$$

where i and j run over the number of spikes in x_1 and x_2 , respectively. Note that by putting the definition of the kernel in equation (5) into equation (4) and using $\phi(x_i) = (h * x_i)(t)$, the decision function is given by

$$\hat{y} = \text{sign} \left(\sum_{i=1}^m \alpha_i k(x_i, x) + b \right) = \text{sign} \left(\int_0^T w(t) \cdot (x * h)(t) dt + b \right) \text{ with } w(t) = \sum_{i=1}^m \alpha_i \phi(x_i).$$

This means that the decision function is equivalent to integrating a weighting function w against the spike train x convolved with h . The weighting function $w(t)$ can be plotted to find epochs within the spike train that strongly influence the decision of the classifier (figure 9).

For analyzing the prediction performance of populations, we generated a kernel on the population by summing the kernel values of the constituent neurons. For example, assume we have trials from a population consisting of an ampullary (a), a P-unit (p), and a T-unit (t), the kernel between the first and the second trial from that population was computed as

$$k((x_1^{(a)}, x_1^{(p)}, x_1^{(t)}), (x_2^{(a)}, x_2^{(p)}, x_2^{(t)})) = k(x_1^{(a)}, x_2^{(a)}) + k(x_1^{(p)}, x_2^{(p)}) + k(x_1^{(t)}, x_2^{(t)}).$$

This is equivalent to stacking the feature vectors $\phi(x^{(a)})$, $\phi(x^{(p)})$, and $\phi(x^{(t)})$ to obtain a combined feature vector $\phi((x^{(a)}, x^{(p)}, x^{(t)}))$.

To find the parameters α_i, b for a given dataset, we used the SVM implementation included in the Python package `sklearn` (Pedregosa et al., 2011). Before training, all data points $\phi(x_i)$ were centered on the mean over the training set. This can be done implicitly on the matrix $K = (k(x_i, x_j))_{ij}$, $1 \leq i, j \leq m$ of pairwise kernel values (Schölkopf and Smola, 2002). To decrease computational time, we limited the number of baseline trials to 1000. The number of chirp trials was typically around 300.

The training stage of the SVM includes a regularization parameter $C \in \mathbb{R}_+$ that trades off complexity of the decision function (4) against classification accuracy on the training set (Schölkopf and Smola, 2002). We determined the best value for C by running a 5-fold stratified cross validation for each $C \in \{10^{-4}, 10^{-3.5}, \dots, 10^3\}$ and choosing the value with the best average accuracy over folds (Duda et al., 2000). Since the number of trials for the baseline activity and chirp responses were usually not the same, we used additional weighting factors provided by the implementation of the SVM that make a mis-classification of a data point more costly if it comes from the under-represented class (Pedregosa et al., 2011).

To measure how well a chirps can be classified against baseline, we used mutual information (Cover and Thomas, 2006)

$$I[\hat{Y} : Y] = \text{E}_{Y,\hat{Y}} \left[\log_2 \frac{P(Y, \hat{Y})}{P(Y)P(\hat{Y})} \right] \quad (6)$$

between the true Y and the predicted label \hat{Y} , which yields a lower bound on the information that the neural response provides about the presence or absence of a chirp (Quiroga and Panzeri, 2009). The maximally possible value of $I[\hat{Y} : Y]$ is given by $I[Y : Y] = -\langle \log_2 P(y) \rangle_Y \leq 1$ bit and, thereby, depends on the percentages of the particular label in the dataset. Since these percentages can vary depending on how many trials were recorded from that particular neuron, we normalize the mutual information by its maximum $I[\hat{Y} : Y]/I[Y : Y]$ and report this value in percent to make the decoding performance comparable between neurons and subjects.

In order to estimate (6) from a finite number of data points, we first estimated the joint distribution $P(\hat{Y} : Y)$ via the relative frequency of the different value combinations of $(y, \hat{y}) \in \{-1, 1\}^2$ on a stratified test set consisting of 20% of the trials withheld from the SVM during the training stage. Afterwards we obtained $P(Y)$ and $P(\hat{Y})$ via marginalization and plugged the resulting distributions into equation (6). To assess the variability of the mutual information estimates, we resampled training and test sets ten times, and repeated the SVM training procedure along with the subsequent mutual information estimation.

3 Results

Frequency modulations in response to mimicks of conspecifics. We characterized the electric communication of *E. virescens* in behavioral experiments. Animals were stimulated with sinusoidal electrical signals mimicking conspecifics with a range of EOD frequencies. All animals performed a two-sided jamming avoidance response (JAR) in which they increased their EOD frequency upon negative difference frequencies and *vice versa* as described in the literature (Watanabe and Takeda, 1963; Bullock et al., 1972; Heiligenberg, 1980, 1991), indicating that they responded to stimulation as they would do to conspecifics. All tested animals showed a JAR but individual differences in the response strength could be observed.

In 16 out of 60 chirp-chamber experiments the tested individuals produced brief frequency modulations. The most common ones are exemplified in figure 1. 73.7% of these frequency excursions were decreases of the EOD frequency, i.e. interruptions. Since they were almost exclusively produced upon stimulation (figure 1E) we interpreted them as communication signals. The chirps consisted of EOD interruptions as well as single cycles of increased frequency (arrows in figure 1 A, E). The most common modulations observed were EOD interruptions of one cycle length, which we termed single-cycle interruptions (figure 1A). Interruptions of single-cycle length occurring in multiple repetitions (effectively decreasing the EOD frequency to half its baseline value, figure 1B) were frequently observed as well. We refer to these patterns as type B chirps to distinguish them from the long-lasting complete interruptions that are not interspersed by EODs and have previously been described (Hopkins, 1974b; Hagedorn and Heiligenberg, 1985), that we call “type A” chirps. In our experiments, we observed a few interruptions lasting longer than one EOD cycle (figure 1C), but never as long as previously described type A chirps (figure 1F). In many cases, chirps were more complex combinations of the three described patterns, often interrupted by a few baseline EOD cycles (figure 1D). During all types of interruptions, the negative offset of the EOD remained, while the counterbalancing positive peaks were missing, thus giving rise to low-frequency components in the signal (figure 1).

The effect of chirps on the electric field of a receiving fish. To characterize how chirps are encoded by the three types of electroreceptors we performed *in vivo* electrophysiological

experiments in which we stimulated the fish with simplified reconstructions of chirps. We investigated which features of the observed frequency modulations are relevant for the sensory perception of communication signals and whether chirps would be discriminable in the sensory domain.

Reconstructions of type B chirps observed in the behavioral experiments, as well as type A chirps described in the literature (Hopkins, 1974a; Hagedorn and Heiligenberg, 1985) (figure 2) were presented to the animal. These chirps were embedded in mimicks of a second fish's EOD that led to beat frequencies of 24 Hz and 100 Hz. During the inter-chirp intervals the receiving fish was thus stimulated with the continuous amplitude modulation caused by the foreign EOD. Chirps interrupt this continuous beat (figure 2A) which led to changes in the beat and the low-frequency content of the stimulus. The beat is phase shifted by the chirps as described before for other species of weakly electric fish (Benda et al., 2005, 2006). The chirp induced phase shifts led to EOD amplitude modulations (rising and falling flanks) that were stepper than those during the beat. This is particularly true if the interruption occurred in early phases of the rising or falling flanks of the beat cycle. The beat phase at which the chirps occurred heavily influenced the amplitude modulation for short interruptions (first, second, and fourth column in figure 2 B). For long interruptions, the phase relation was not relevant (third, and fifth column in figure 2 B). Cessation of EODs during chirps further induced low-frequency shifts of the stimulus that drove ampullary receptors. In contrast to P-units and T-units, however, these are generally independent of the beat phase in which the chirp occurs (grey lines in figure 2 B).

In the following paragraphs we show the responses of P-units, T-units, and ampullary receptors to the different chirp stimuli.

P-units respond to amplitude modulations during chirps with a change in firing rate and synchrony. P-unit electroreceptors encode amplitude modulations of the fish's own EOD in the modulation of their firing rate: the firing rate increases upon amplitude increases and *vice versa*. Correspondingly, the firing rate of P-units was sinusoidally modulated in response to stimulation with beats only (figure 3B). Chirps that lead to increases in EOD amplitude induced a firing rate increase exceeding the maximum firing rate during the beat. If the chirp led to decreases in EOD amplitude, the firing rate also decreased (figure 3B). In addition, chirps also

influenced the synchrony of P-unit responses. Sudden changes in amplitude modulation led to high degrees of synchrony across multiple repetitions of the same stimulus, which can be regarded as a proxy for the responses of multiple neurons in the receptor population (Benda et al., 2005). As shown in figure 2 the phase relation between chirp and underlying beat strongly influenced the EOD amplitude modulation, hence, subsequent analysis was performed for each phase relation separately.

Different response features were evaluated and compared between the chirp (*chirp response*), the corresponding beat phase (*beat response*), as well as the response to a complete beat cycle (*control response*), in order to quantitatively analyse of the effects of chirps on the P-units.

During single-cycle interruptions in a 24 Hz beat, the mean firing rate was sinusoidally modulated around the average firing rate across chirp phases (figure 4A, first column). It was shifted with respect to the firing rate during the beat in most phases. The response synchrony, evaluated as the correlation across trials, was higher during the *chirp response* than during *beat-* and *control responses* in many chirp phases (figure 4A, middle panel). Moreover, the firing rate of P-units changed more rapidly in response to chirps than it did in response to the beat, as evaluated by the derivative of the firing rate (figure 4A, bottom panel).

With an increasing duration of type B chirps, synchrony in the *chirp response* increased and was substantially higher than both the *beat-* and *control response* across all phases (figure 4A, second and third column). The derivatives of the firing rate increased significantly above beat and control values as well. For long type B chirps, the firing rate did not differ from beat and control values, because P-units responded with alternating increases and decreases in firing rate, averaging out over the course of the chirp.

Type A chirps had similar effects on the firing rate as type B chirps (figure 4A, fourth and fifth column). The longer the interruption, the less the firing rate modulation across phases and the smaller the difference between *chirp response* and *beat response*, as well as the *control response*.

In contrast to type B chirps which increased response synchrony, type A interruptions reduced synchrony significantly. This effect was stronger the longer the interruption lasted (compare figure 4A, middle panels).

Both upon long type A and type B chirps, P-units responded to the modulation generated at

the onset (figure 4B) and offset of the chirp with a modulation in firing rate similar to single cycle interruptions, because at onset and offset all chirp types generated the same abrupt changes in EOD amplitude.

The frequency and sign of the beat did not alter P-unit responses to chirps qualitatively. Chirps embedded in a 100 Hz beat led to qualitatively similar, yet weaker responses compared to 24 Hz beats (figure 5). Because the amplitude modulations of the fast beat alone were already quite effective in driving the neurons to their firing rate limits, changes caused by the chirps had less impact. The spike-train correlation and the PSTH derivatives upon long type A chirps decreased much stronger at 100 Hz than at 24 Hz beats, because the firing was stronger correlated during fast than during slow beats and therefore interruptions had a stronger decorrelating effect. In fast beats, the mean firing rate upon long type A and type B chirps was not modulated with respect to the beat, which was similar to slow beats.

The quality of P-unit responses to chirps was independent of the sign of the beat. Chirps embedded in a 24 Hz beat of negative difference frequencies (i.e., the receiving fish has a higher EOD frequency than the fish producing the chirps) led to qualitatively very similar responses as chirps in positive beats of the same frequency.

Heterogenous P-unit responses. Although general response patterns could be extracted for all P-units, there was a substantial amount of heterogeneity in the responses (see error bars in figures 4 and 5), due to the heterogeneity of P-units in their baseline firing rate. P-units with a very high baseline firing rate close to the EOD frequency were not able to increase their firing frequency substantially upon amplitude upstrokes caused by chirps, thus, their response was much more pronounced to chirps causing downstrokes of the EOD amplitude. The opposite was true for P-units with very low baseline firing rates (shown in figure 6 for two example cells).

T-units respond to chirps with changes in spike timing. T-units are the second receptor type of the tuberous electrosensory system that are driven by the fish's own EOD and fire one spike in a phase-locked manner to every EOD cycle. Thus, encoding of chirps in the firing rate is not possible. However, it has been reported that T-units encode phase modulation during beats

in their spike timing (Bastian and Heiligenberg, 1980; Rose and Heiligenberg, 1986; Lytton, 1991; Fortune et al., 2006). Therefore, we analysed the inter-spike intervals (ISIs) of T-units as a measure of spike timing, as well as the correlation of ISIs across stimulus repetitions.

T-units showed modulations of their ISIs in response to chirps (figure 3A). Upon single cycle interruptions, their ISIs decreased if the interruption generated a rising flank in amplitude and increased if it generated a falling flank (figure 3C). The positive and negative deflections of the mean ISI were larger during chirps than during the beat.

A pattern very similar to P-units emerged when analysing T-unit ISIs and their correlation across trials for the different chirp types: for single-cycle interruptions, the ISIs were sinusoidally modulated around the control across phases, and shifted in phase with respect to the *beat response* (figure 3B). The correlation of ISIs across trials was higher than the correlation during the beat in a few phases only. With increasing length of type B interruptions, the ISI modulations relative to the beat decreased, but the correlation in ISIs between trials increased. Upon longer type A chirps both the ISI modulations and the correlation across trials were not different from the beat values (figure 7A).

Similar to P-units, T-units also modulated their ISIs at the beginning and end of a chirp irrespective of chirp type (figure 7B).

Ampullary receptors respond to low-frequency components of all chirp types. Ampullary receptors belong to the passive electrosensory system and are tuned to low-frequency modulations in the electric field. When the EODs of two fish interact in a communication context, the receiving fish's EOD is amplitude modulated (compare figure 2 A). Ampullary receptors are not driven by this AM (figure 3 D, period before chirp onset). During the chirp, however, when the chirping fish ceased generating the positive deflections of its EOD, the negative DC component prevails and induces low-frequency signals (solid black lines in figure 1 and gray lines in figure 2 B) which drive the ampullary receptors. The neurons responded to the chirps with an increase in firing rate (figure 3D).

Since ampullary receptors are not driven by the fish's own EOD and its amplitude modulation, the phase relation of chirp and beat is not relevant and data was pooled across phases. Ampullary receptors encoded the duration of the chirp with the duration of their response (fig-

ure 8A). With increasing duration of the interruption, the difference between *chirp response* and *control response* increased in a linear way (figure 8B). However, type A interruptions triggered larger ampullary responses than type B interruptions of similar length, corresponding to their different low-frequency contents (figure 8B). Moreover, the modulation of the firing rate, calculated as the firing rate derivative, was stronger during chirps than during the beat (figure 8C), as was the firing synchronicity calculated as the spike train correlation (figure 8D). For both measures, the responses were stronger for type A than type B chirps, irrespective of the strength of the low frequency content.

Decoding analysis P-unit, T-units, and ampullary cells extract different features from the different chirp types. This suggests that a potential read-out mechanism might benefit from the joint information contained in the different receptors for detecting and identifying these communication signals. To quantify how much information each cell type contains about each chirp type, we used a decoding approach in which we train a machine learning algorithm to distinguish between chirp and baseline responses based on the neural responses of single neurons or small populations to chirps.

We trained a support vector machine classifier (SVMs; Boser et al., 1992; Cortes and Vapnik, 1995) for each cell and each chirp type to predict whether a given trial was the mere baseline response or the response to a chirp. Baseline activity data points were randomly selected windows of activity from parts of the trials where only a beat was present, whereas chirp data points were extracted directly after the onset of the chirp. We defined the window length for each fish in terms of EOD cycles to provide a fair comparison between individuals with different EOD frequencies. SVMs were trained for window lengths of 5, 10, 20, 25, and 30 EOD cycles.

For single neurons, the SVM yielded a decision rule of the form

$$\hat{y} = \text{sign} \left(\int_0^T w(t) \cdot (x * h)(t) dt + b \right), \quad (7)$$

where T is the length of the time window extracted after the chirp onset, and $(x * h)(t)$ is the spike train convolved with a one-sided exponential $h(t) = [t]_+ \exp(-t/\tau)$. We use this particular filter kernel to simulate the membrane potential of a pyramidal cell post-synaptic to the receptors. $w(t)$ and b are a weighting function and an offset, respectively, which are optimized by the SVM to produce a positive response if the neural activity x results from a spike and negative if

it corresponds to baseline activity. Therefore, \hat{y} is the predicted label of the tested spike train x . In the following, we denote the true label with y .

We found that the weighting functions $w(t)$ were similar to the difference between the means over the convolved trials for chirp and baseline activity (figure 9, second to fourth panel in A–C). This is expected since $w(t)$ should emphasize regions in which the two conditions are most distinguishable.

As in our analyses above, neural response changes were triggered by particular features of the chirps. For instance, P-units and T-units changed their activity upon omitted EOD cycles in type B chirps (figure 9, A and B), whereas ampullary cells mostly responded to the long pauses of type A chirps (figure 9, C). Therefore, we expected that responses of ampullary units yield more information about A-type chirps, while T-units and P-units should perform better in predicting the presence of type B chirps.

We quantified the decoding performance by the mutual information $I[Y, \hat{Y}]$ between the true and the predicted labels normalized by the maximally achievable mutual information (see methods). Because of the data-processing inequality (Cover and Thomas, 2006), the mutual information $I[Y, \hat{Y}]$ is a lower bound on the available information about chirp vs. baseline in the neural responses (Quiroga and Panzeri, 2009). The mutual information was estimated for each neuron, each chirp type, and each window length from the predictions on a stratified test set consisting of 20% of the data points not used for training the SVM.

The mutual information increased with increasing number of EOD cycles available to the classifier (figure 9, A–C). For most cells, it saturated at around 15–20 EODs. Across all neurons the decoding performance was quite variable (figure 10), often shifting to higher percentages with increasing window lengths. P-units generally performed well on all chirp types, but better on type B (figure 10, first row). T-units also performed better on type B chirps, but did not reach the same performance levels as P-units or ampullary cells (figure 10 second row). Ampullary units performed better on type A chirps, in particular on the long A20 chirp (figure 10, third row). Generally, all cells yielded most information for longer chirps of their preferred type.

The fact that ampullary units yield more information about type A chirps while P-units and T-units perform better on type B chirps suggests that a potential read-out mechanism could benefit from looking at all cell types at once. To quantify this, we assembled several populations

consisting of three cells recorded from the same individual. One set of populations consisted of all cell types (figure 10, APT), while the other set consisted of different P-units only (figure 10, PPP). For populations, the decision function of the SVM (equation (7)) obtained an integral term for each member cell. In the finite dimensional case, this would be equivalent to stacking the feature vectors of all neurons in the population.

Populations generally yielded more information about baseline vs. chirp responses than single units. However, except for the A20 chirp, the PPP population performed better than the mixed APT population. For the A20 chirp, the APT population yielded more information than the PPP population ($p \leq 0.006$, two independent sample t-test, Bonferroni corrected for five comparisons).

4 Discussion

We investigated the neural representation of communication signals (chirps) in the parallel channels of the electrosensory system of *Eigenmannia virescens*. In a first step we categorized the different communication signals recorded in behavioral experiments leading to the description of a previously unknown chirp type. Next, we characterized the neural representation of each chirp type in all three electroreceptor afferents and find that each type of electroreceptor extracts a distinct set of features. For P- and T-units these features were more pronounced for type B chirps while they were more distinctive for type A chirps in ampullary units. A subsequent decoding analysis on small populations of receptors suggests that a potential read-out mechanism should use this complementary information of the parallel sensory channels for a reliable chirp detection.

A new chirp type. *Eigenmannia* communication signals have been described as EOD interruptions of several tens to hundreds milliseconds duration (Hopkins, 1974a; Hagedorn and Heiligenberg, 1985). We termed these type A chirps. In our behavioral experiments we did not observe such chirps. Rather, we recorded rapid excursions in the EOD frequency which consisted of single-cycle EOD interruptions or multiple repetitions of single-cycle interruptions that have not been described before (figure 1A-D).

Type A chirps are closely related to mating behavior and are therefore considered social signals (Hagedorn and Heiligenberg, 1985). For several reasons we believe that the type B chirps observed here can also be considered as social signals.

1. They were almost exclusively observed upon stimulation with external electric fields which mimicked conspecifics (figure 1 E).
2. Qualitatively, they were similar to previously described chirps, since they were also decreases of the EOD frequency. Some of the longer chirps (figure 1 D) resembled previously described “incomplete interruptions” (Hagedorn and Heiligenberg, 1985). Interestingly, stimulation of the pre-pacemaker nucleus (PPN, Kawasaki and Heiligenberg, 1988; Kawasaki et al., 1988) and the preoptic area (PEO, Wong, 2000) leads to EOD modulations similar to the interruptions described in this study.

Why did we not observe long (type A) interruptions which so closely became associated with *E. virescens* communication? The main reason may be that previous observations were mostly conducted on sexually mature animals during tuberous courtship behavior (Hagedorn and Heiligenberg, 1985; Hopkins, 1974a). Hopkins (1974a) shows that chirps during the breeding season are distinctly longer and are produced in higher numbers than outside the season.

It is therefore conceivable that shorter EOD interruptions are produced by *E. virescens* outside of the breeding season and possibly act as negotiation of threat signals similar to type 2 chirps in *A. leptorhynchus* (Engler and Zupanc, 2001; Hupé et al., 2008), while long interruptions are produced by males in the context of courtship behavior.

Coding of chirps in three types of electroreceptors. If we assume that the different chirp types are of behavioral importance and have distinct meanings, the nervous system must be able to identify them on the basis of the electroreceptor responses. We therefore assessed how the two types of chirps are encoded in the spiking responses of the primary afferents of the three types of electroreceptors. We characterized the effects of chirps on different aspects of the neuronal responses: the firing rate (or the interspike-interval in T-units), the spike time correlation as a measure of synchronicity, and the amount of change in the firing rate.

Synchrony is a good code for chirp types in P-units. Single-cycle interruptions as well as short type A and B chirps lead to modulations of the P-unit firing rate around the average firing rate depending on the phase relation between beat and chirp (figure 4). This ambiguity renders the firing rate an inapt measure for the decoding of the neuronal responses. The level of response synchrony, however, was distinctly different between type A and type B chirps. Further, the changes in response synchrony were robust against changes in the phase relation between chirps and the underlying beat. On the basis of this feature type A chirps on the one hand and type B chirps and single-cycle interruptions, on the other, could be separated. This encoding scheme is surprisingly similar to a related weakly electric fish, the brown ghost knife fish, *Apteronotus leptorhynchus*. In this species, different types of chirps are encoded in P-unit synchronization and de-synchronization as well (Benda et al., 2006; Walz et al., 2014), despite the very different nature of the communication signals which are transient increases in EOD frequency and do not contain low-frequency components.

The responses of P-units of *E. virescens* were qualitatively similar for slow and fast beats (compare figures 4 and 5), as well as for negative beats. In *A. leptorhynchus*, however, chirps can have opposing effects on P-unit responses, depending on the beat frequency (Benda et al., 2006; Hupé et al., 2008; Walz et al., 2014). In this species, sexual dimorphism in EOD frequency is very pronounced and EOD frequency is correlated with sex (Dunlap et al., 1998). Therefore beats in intersexual encounters are likely of the same sign. In *E. virescens*, however, there is only a statistical correlation between sex and EOD frequency (males tend to have lower frequencies than females), and this is most pronounced in sexually mature animals (Hopkins, 1974a). Recordings show that males that chirp vigorously during courtship behavior could even have higher EOD frequencies than their accompanying females (figure 7 in Hopkins, 1974a and figure 5 in Hagedorn and Heiligenberg, 1985). It is therefore likely that chirps often occur in beats of different signs and thus an encoding scheme that is largely independent of the beat appears appropriate in *E. virescens*.

T-units can encode chirp features in their spike timing. T-units are driven by the fish's own EOD and fire one spike to each discharge of the electric organ. They encode the phase of the beat in their spike timing, which can be compared across different body areas and the phase modulations can be extracted (Bastian and Heiligenberg, 1980; Rose and Heiligenberg, 1986; Lytton, 1991; Fortune et al., 2006). T-units have been shown to respond to self-generated chirps by ceasing to fire during the interruptions because there was no EOD present (Metzner and Heiligenberg, 1991). We give the first account of T-units responding to chirps in a receiving fish. Since the receiver's EOD was still present, T-units continuously fired action potentials during the chirps (figure 3B) and the firing rate therefore is uninformative. However, chirps generated modulations of inter spike intervals (ISIs, figure 3B). Type B chirps generated the strongest ISI modulations while type A chirps were only marked by brief changes in the ISI mostly at the beginning. Similar to P-units, these ISI modulations were strongly correlated across trials especially upon type B, but not type A chirps (figure 7). Reading out the modulation of the ISIs of T-units may thus support the discrimination between type A and type B chirps.

Ampullary responses encode the duration of chirps. The firing rate and response synchrony of ampullary receptors increased in response to all types of chirps compared to the control. This

is in accordance with observations on ampullary responses to self-generated chirps (Metzner and Heiligenberg, 1991). The response strength was correlated to the amount of low-frequency content (figures 3, 8B). However, the response to short type A chirps was stronger than to long type B chirps, even though the latter had a stronger absolute low-frequency component. We found the same pattern for the derivative of the firing rate, as well as the firing synchrony (figure 8C,D). Therefore, it is hard to conceive how ampullary receptors could encode the chirp type in the modulation of their firing rate. Moreover, the strength of low-frequency content does not only depend on the type of chirp, but also on how close the chirping fish is to the receiver, which makes encoding of chirp types via the firing rate even more ambiguous. Ampullary receptors could, however, encode the duration of a chirp in the duration of their response (figure 8A). Thus, while it is not possible to discern chirp types unambiguously from ampullary responses, the occurrence and duration of the chirp is reliably encoded.

Decoding of *Eigenmannia* communication signals. It is likely that the different chirp types have different behavioral meanings in social encounters of the fish. Therefore, reliably distinguishing these communication signals is crucial perceptual task for the animal. Our results show that communication signals are encoded by all three types of electroreceptors. Chirps can consist of combinations of longer and shorter interruptions (figure 1 D) which cause characteristic response profiles in each receptor type (figure 3).

Depending on the chirp type certain receptors are better suited to detect certain their presence than others (figure 10 A, P, T). The most prominent feature of long type A chirps—the putative courtship signals—is their strong low-frequency component, which causes little firing rate modulation and de-synchronization in P-and T-units, but strong increases in firing rate and synchronization in ampullary receptors. Type B chirps—possible negotiation signals—on the other hand, are characterized by strong firing rate modulation and synchronization in P-units and T-units, while the weaker low-frequency component induces less pronounced changes in ampullary responses. Our single-unit decoding analysis confirms that type B chirps are better detected in P- and T- units while ampullary response provide more information about type A chirps (figure 10 A, P, T).

However, any chirp contains features that drive both the tuberous and the ampullary system

at the same time. This suggests that a potential read-out mechanism could benefit from combining information from all electroreceptor types in at least two ways: Both systems are subjected to environmental noise from various sources (Metzner and Heiligenberg, 1991; Benda et al., 2013) and integration of the tuberous and the ampullary system could improve the robustness of detection. Moreover, combining information from different receptor types could reduce ambiguities. The population decoding analysis (figure 10, APT, PPP) demonstrates that chirps can be detected more faithfully from the response of several receptors. For most chirp types detection performance based on P-units activity alone turned out to be superior to that of the single-unit or mixed population. Chirps with long interruptions, however, are more reliably decoded by mixed populations of the tuberous and ampullary receptors. However, type A chirps have been reported with durations in the range from 100 ms up to 2 s (Hopkins, 1974b; Hagedorn and Heiligenberg, 1985) which is considerably larger than the longest type A chirp we used (A 20). Therefore, the fact that it is only this chirp that is more reliably detected by the mixed population could simply be a consequence of the limited stimulus set which would mean that our analysis rather underestimates the importance of parallel processing in tuberous and ampullary system. We therefore conclude from our results that the type B negotiation signals could be well decoded on the basis of P-units alone, while the detection of courtship signals (type A chirps) clearly profits from combining ampullary and P-unit responses. Combining information from these parallel channels can reduce ambiguity in the signals, and make encoding more robust.

5 Acknowledgements

We thank Rüdiger Krahe for his help establishing *Eigenmannia* recordings in our lab, and Henriette Walz and Janez Prešern for comments and discussion. J.B. and J.G. are supported by BMBF grant 01GQ0802 to J.B.. F.S. is partly funded by Bernstein Center for Computational Neuroscience Tübingen (BMBF grant 01GQ1002).

References

- Bastian J, Heiligenberg W.** Neural correlates of the jamming avoidance response of *Eigemannia*. *J Comp Physiol A* 136: 135–152, 1980. ISSN 0340-7594.
- Bastian J, Schniederjan S, Nguyenkim J.** Arginine vasotocin modulates a sexually dimorphic communication behavior in the weakly electric fish *Apteronotus leptorhynchus*. *J Exp Biol* 204(Pt 11): 1909–1923, 2001.
- Benda J, Grewe J, Krahe R.** Neural noise in electrocommunication: From burden to benefits. In: *Animal Communication and Noise*, edited by **Brumm H**, volume 2 of *Animal Signals and Communication*, pages 331–372. Springer Berlin Heidelberg, 2013. ISBN 978-3-642-41493-0.
- Benda J, Longtin A, Maler L.** Spike-frequency adaptation separates transient communication signals from background oscillations. *J Neurosci* 25(9): 2312–2321, 2005.
- Benda J, Longtin A, Maler L.** A synchronization-desynchronization code for natural communication signals. *Neuron* 52(2): 347–358, 2006.
- Bensmaia SJ.** Tactile intensity and population codes. *Behav Brain Res* 190(2): 165–173, 2008.
- Boser BE, Guyon IM, Vapnik VN.** A Training Algorithm for Optimal Margin Classifiers. In: *Proceedings of the 5th Annual ACM Workshop on Computational Learning Theory*, pages 144–152. 1992. ISBN 089791497X. ISSN 0-89791-497-X.
- Bullock T, Hamstra R, Scheich H.** The jamming avoidance response of high frequency electric fish. *J Comp Physiol A* 77: 1–22, 1972. ISSN 0340-7594.
- Bullock TH, Chichibu S.** Further analysis of sensory coding in electroreceptors of electric fish. *Proc Natl Acad Sci U S A* 54(2): 422–429, 1965.
- Cortes C, Vapnik V.** Support-vector networks. *Machine Learning* 20(3): 273–297, 1995. ISSN 0885-6125.
- Cover TM, Thomas JA.** *Elements of Information Theory 2nd Edition (Wiley Series in Telecommunications and Signal Processing)*. Wiley-Interscience, 2006. ISBN 0471241954.

Duda RO, Hart PE, Stork DG. *Pattern Classification (2nd Edition)*. Wiley-Interscience, 2000.
ISBN 0471056693.

Dunlap KD, Oliveri LM. Retreat site selection and social organization in captive electric fish, *Apteronotus leptorhynchus*. *J Comp Physiol A Neuroethol Sens Neural Behav Physiol* 188(6): 469–477, 2002.

Dunlap KD, Thomas P, Zakon HH. Diversity of sexual dimorphism in electrocommunication signals and its androgen regulation in a genus of electric fish, *Apteronotus*. *J Comp Physiol A* 183: 77–86, 1998. ISSN 0340-7594.

Dye J. Dynamics and stimulus-dependence of pacemaker control during behavioral modulations in the weakly electric fish, *Apteronotus*. *J Comp Physiol A* 161(2): 175–185, 1987.

Engler, Zupanc. Differential production of chirping behavior evoked by electrical stimulation of the weakly electric fish, *Apteronotus leptorhynchus*. *J Comp Physiol A* 187: 747–756, 2001. ISSN 0340-7594.

Fortune ES, Rose GJ, Kawasaki M. Encoding and processing biologically relevant temporal information in electrosensory systems. *J Comp Physiol A* 192(6): 625–635, 2006.

Hagedorn M, Heiligenberg W. Court and spark: electric signals in the courtship and mating of gymnotoid fish. *Anim Behav* 33(1): 254 – 265, 1985. ISSN 0003-3472.

Heiligenberg W. The jamming avoidance response in the weakly electric fish *Eigenmannia*. A behavior controlled by distributed evaluation of electroreceptive afferences. *Naturwissenschaften* 67(10): 499–507, 1980.

Heiligenberg W. *Neural nets in electric fish*. MIT Press, 1991.

Hopkins CD. Electric communication: Functions in the social behavior of *Eigenmannia virescens*. *Behaviour* 50(3/4): 270–305, 1974a.

Hopkins CD. Electric communication in the reproductive behavior of *Sternopygus macrurus* (Gymnotoidei). *Z Tierpsychol* 35(5): 518–535, 1974b.

Hopkins CD. Stimulus filtering and electroreception: Tuberous electroreceptors in three species of Gymnotoid fish. *J Comp Physiol A* 111: 171–207, 1976. ISSN 0340-7594.

Hunter JD. Matplotlib: A 2d graphics environment. *Computing In Science & Engineering* 9(3): 90–95, 2007.

Hupé GJ, Lewis JE, Benda J. The effect of difference frequency on electrocommunication: Chirp production and encoding in a species of weakly electric fish, *Apteronotus leptorhynchus*. *J Physiol (Paris)* 102(4-6): 164 – 172, 2008. ISSN 0928-4257.

Jones E, Oliphant T, Peterson P, et al. SciPy: Open source scientific tools for Python. 2001.

Kawasaki M, Heiligenberg W. Individual prepacemaker neurons can modulate the pacemaker cycle of the gymnotiform electric fish, *Eigenmannia*. *J Comp Physiol A* 162: 13–21, 1988. ISSN 0340-7594.

Kawasaki M, Maler L, Rose GJ, Heiligenberg W. Anatomical and functional organization of the prepacemaker nucleus in gymnotiform electric fish: the accommodation of two behaviors in one nucleus. *J Comp Neurol* 276(1): 113–131, 1988.

Kramer B. The sexually dimorphic jamming avoidance response in the electric fish *Eigenmannia* (Teleostei, Gymnotiformes). *J Exp Biol* 130(1): 39–62, 1987.

Lytton WW. Simulations of a phase comparing neuron of the electric fish *Eigenmannia*. *J Comp Physiol A* 169(1): 117–125, 1991.

Marsat G, Maler L. Neural heterogeneity and efficient population codes for communication signals. *J Neurophysiol* 104(5): 2543–2555, 2010.

Metzner W, Heiligenberg W. The coding of signals in the electric communication of the gymnotiform fish *Eigenmannia*: from electroreceptors to neurons in the torus semicircularis of the midbrain. *J Comp Physiol A* 169(2): 135–150, 1991.

Nassi JJ, Callaway EM. Parallel processing strategies of the primate visual system. *Nat Rev Neurosci* 10(5): 360–372, 2009.

- Park IM, Seth S, Li L, Principe JC.** Kernel methods on spike train space for neuroscience: a tutorial. *Signal Processing Magazine, IEEE* 30(4): 149 – 160, 2013.
- Pedregosa F, Varoquaux G, Gramfort A, Michel V, Thirion B, Grisel O, Blondel M, Pret-tenhofer P, Weiss R, Dubourg V, Vanderplas J, Passos A, Cournapeau D, Brucher M, Perrot M, Duchesnay E.** Scikit-learn: Machine learning in Python. *Journal of Machine Learning Research* 12: 2825–2830, 2011.
- Quijan Quiroga R, Panzeri S.** Extracting information from neuronal populations: information theory and decoding approaches. *Nat Rev Neurosci* 10(3): 173–185, 2009. ISSN 1471-003X.
- Rose G, Heiligenberg W.** Neural coding of difference frequencies in the midbrain of the electric fish *Eigenmannia*: reading the sense of rotation in an amplitude-phase plane. *J Comp Physiol A* 158(5): 613–624, 1986.
- Scheich H, Bullock TH, Hamstra R Jr.** Coding properties of two classes of afferent nerve fibers: high-frequency electroreceptors in the electric fish, *Eigenmannia*. *J Neurophysiol* 36(1): 39–60, 1973.
- Schölkopf B, Smola AJ.** *Learning with Kernels: Support Vector Machines, Regularization, Optimization, and Beyond (Adaptive Computation and Machine Learning)*. The MIT Press, 2002.
- Tan EW, Nizar JM, Carrera-G E, Fortune ES.** Electrosensory interference in naturally occurring aggregates of a species of weakly electric fish, *Eigenmannia virescens*. *Behav Brain Res* 164(1): 83–92, 2005.
- Todd BS, Andrews DC.** The identification of peaks in physiological signals. *Comput Biomed Res* 32(4): 322–335, 1999.
- Vonderschen K, Chacron MJ.** Sparse and dense coding of natural stimuli by distinct midbrain neuron subpopulations in weakly electric fish. *J Neurophysiol* 106: 3102–3118, 2011.
- Walz H, Grewe J, Benda J.** Static frequency tuning properties account for changes in neural synchrony evoked by transient communication signals. *J Neurophysiol* page accepted, 2014.

Wässle H. Parallel processing in the mammalian retina. *Nat Rev Neurosci* 5(10): 747–757, 2004.

Watanabe A, Takeda K. The change of discharge frequency by a.c. stimulus in a weak electric fish. *J Exp Biol* 40(1): 57–66, 1963.

Wong CJ. Electrical stimulation of the preoptic area in *Eigenmannia*: evoked interruptions in the electric organ discharge. *J Comp Physiol A* 186(1): 81–93, 2000.

Zakon H. The electroreceptive periphery. In: *Electroreception*, edited by **Bullock T, Heiligenberg W**, pages 103 – 156. John Wiley & Sons, New York, 1986.

Zakon HH, Dunlap KD. Sex steroids and communication signals in electric fish: a tale of two species. *Brain Behav Evol* 54(1): 61–69, 1999.

Zakon HH, Thomas P, Yan HY. Electric organ discharge frequency and plasma sex steroid levels during gonadal recrudescence in a natural population of the weakly electric fish *sternopygus macrurus*. *J Comp Physiol A* 169(4): 493–499, 1991.

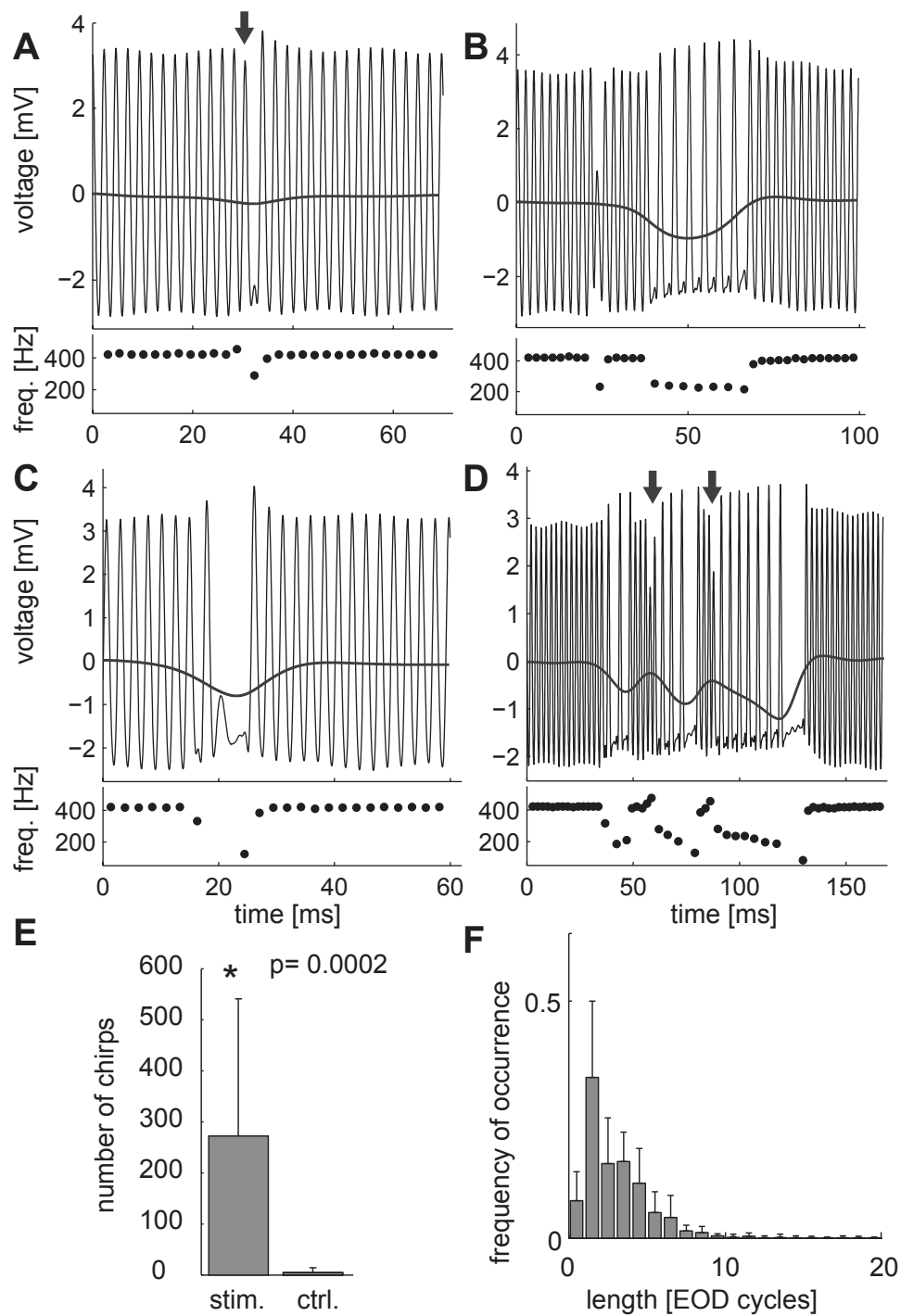


Figure 1

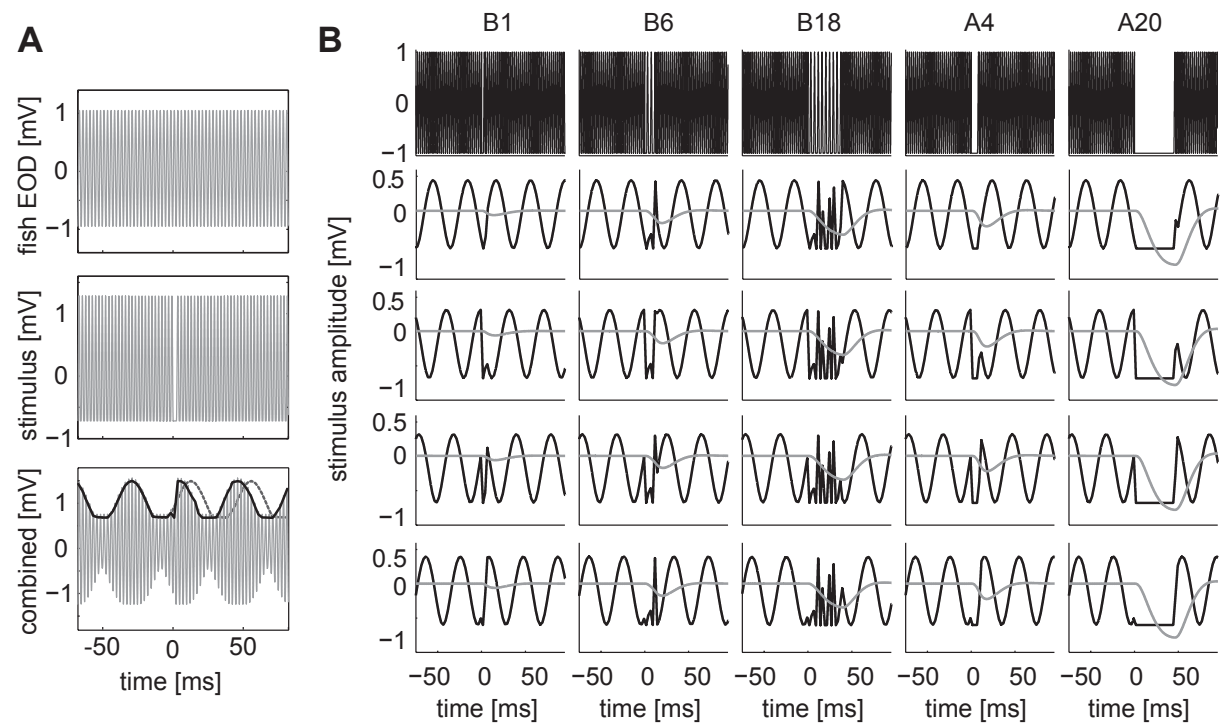


Figure 2

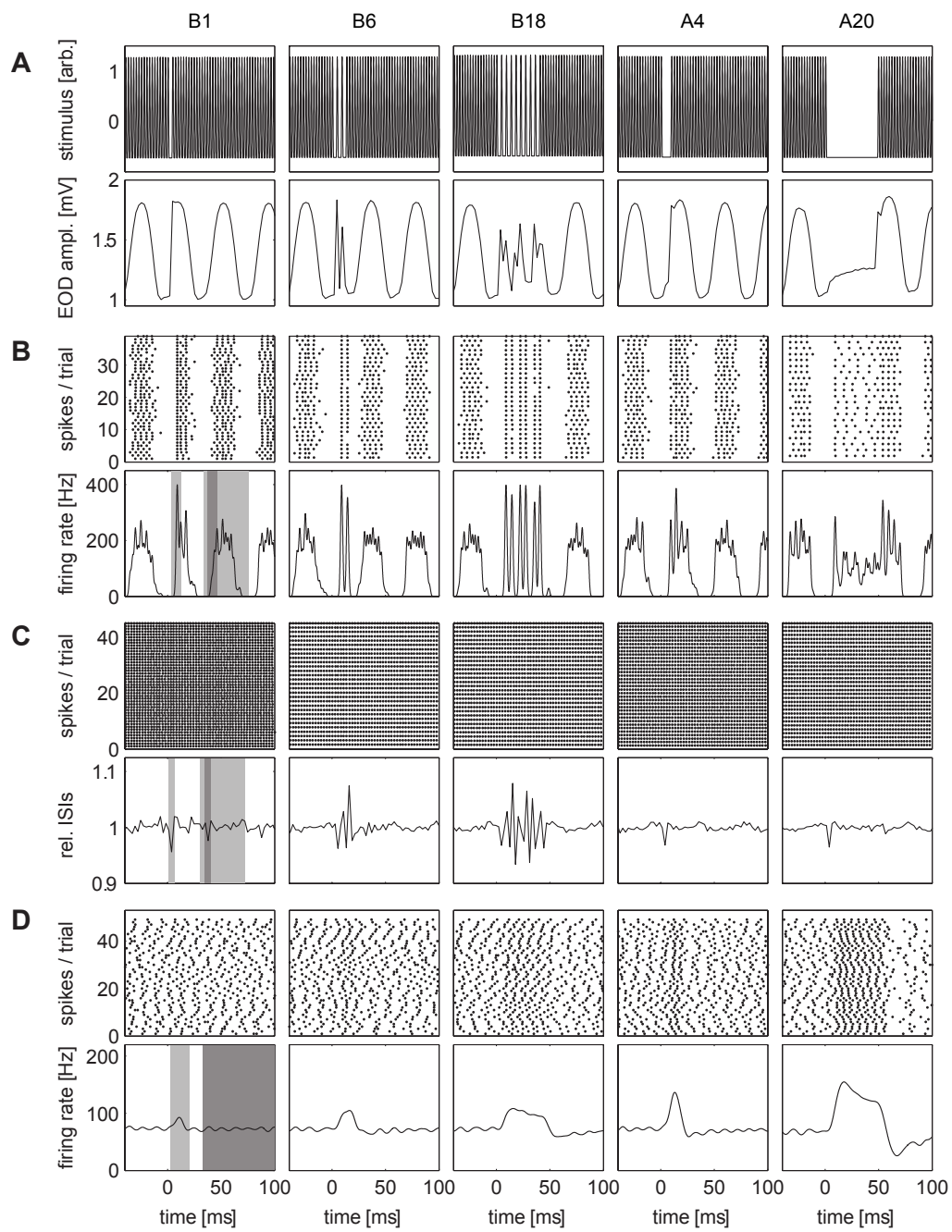


Figure 3

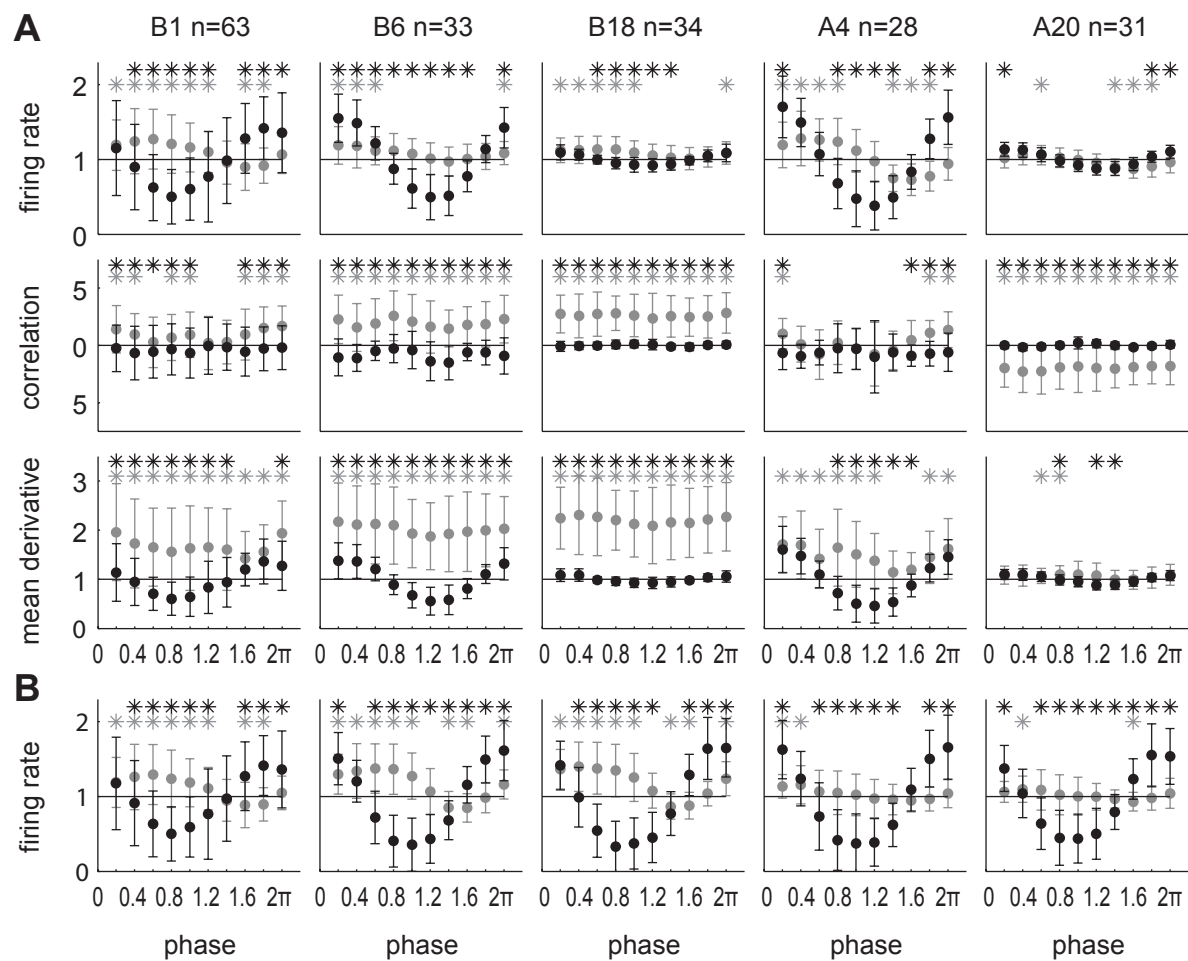


Figure 4

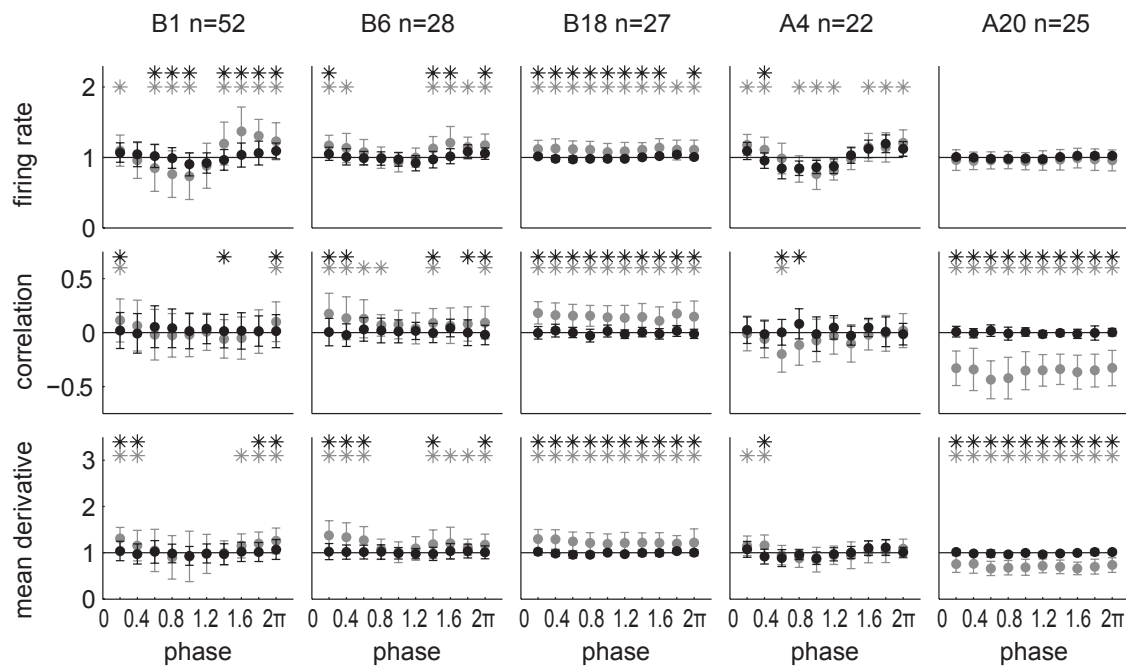


Figure 5

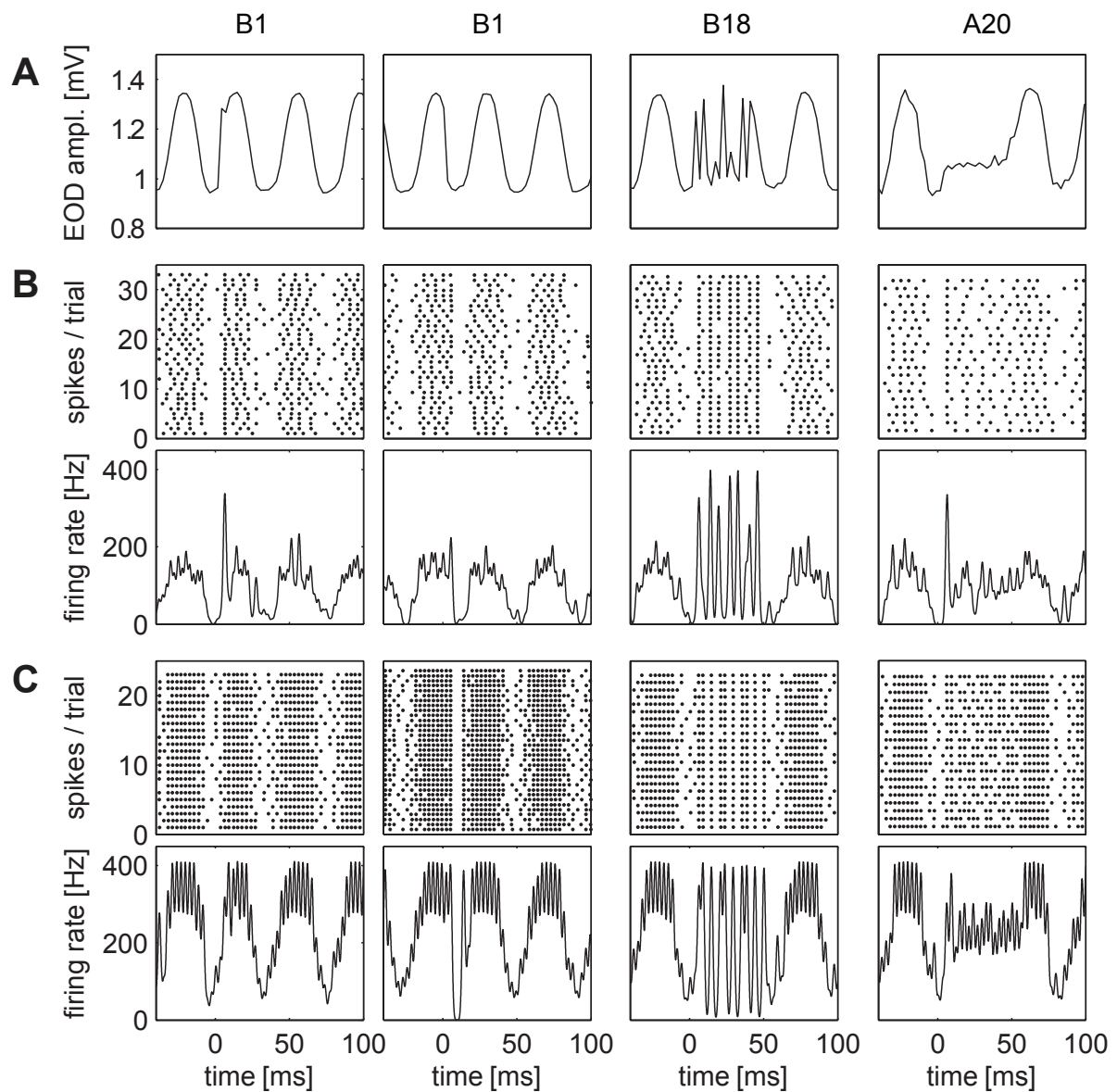


Figure 6

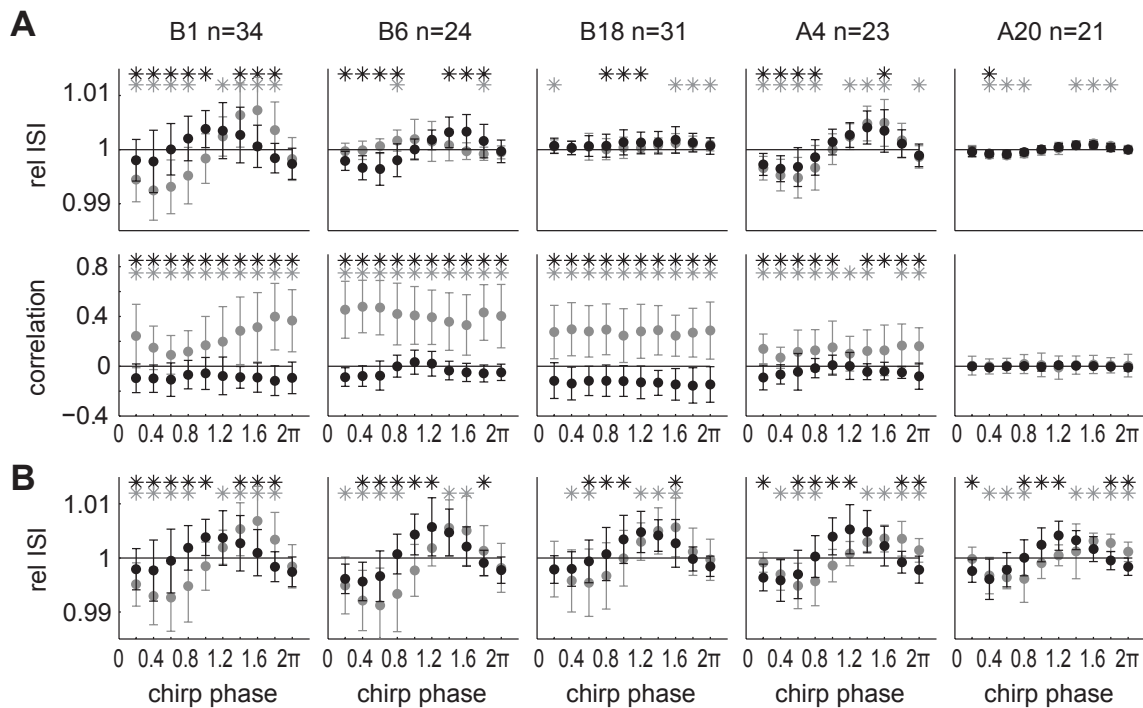


Figure 7

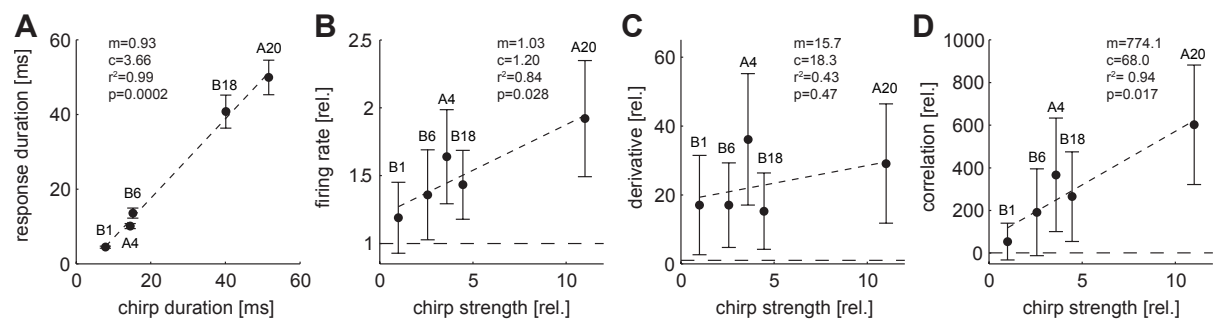


Figure 8

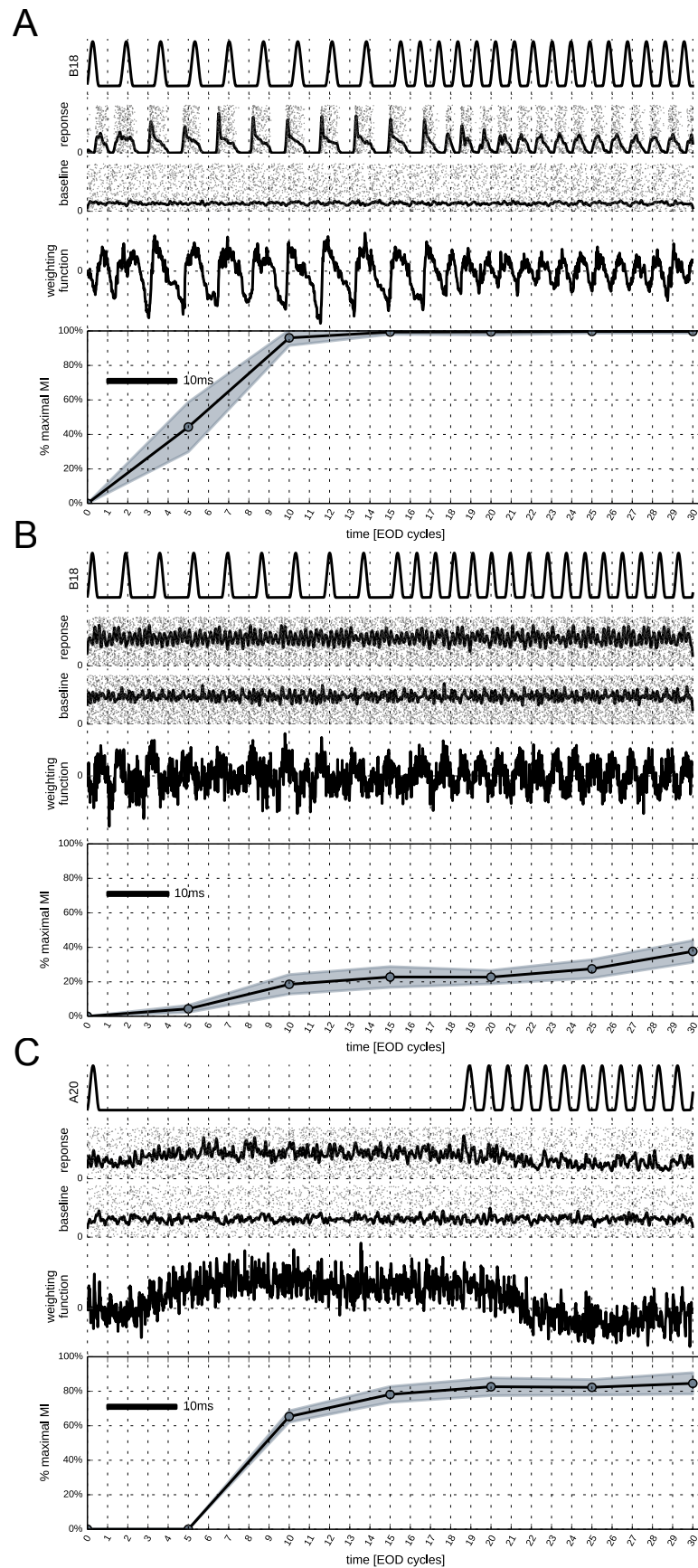


Figure 9

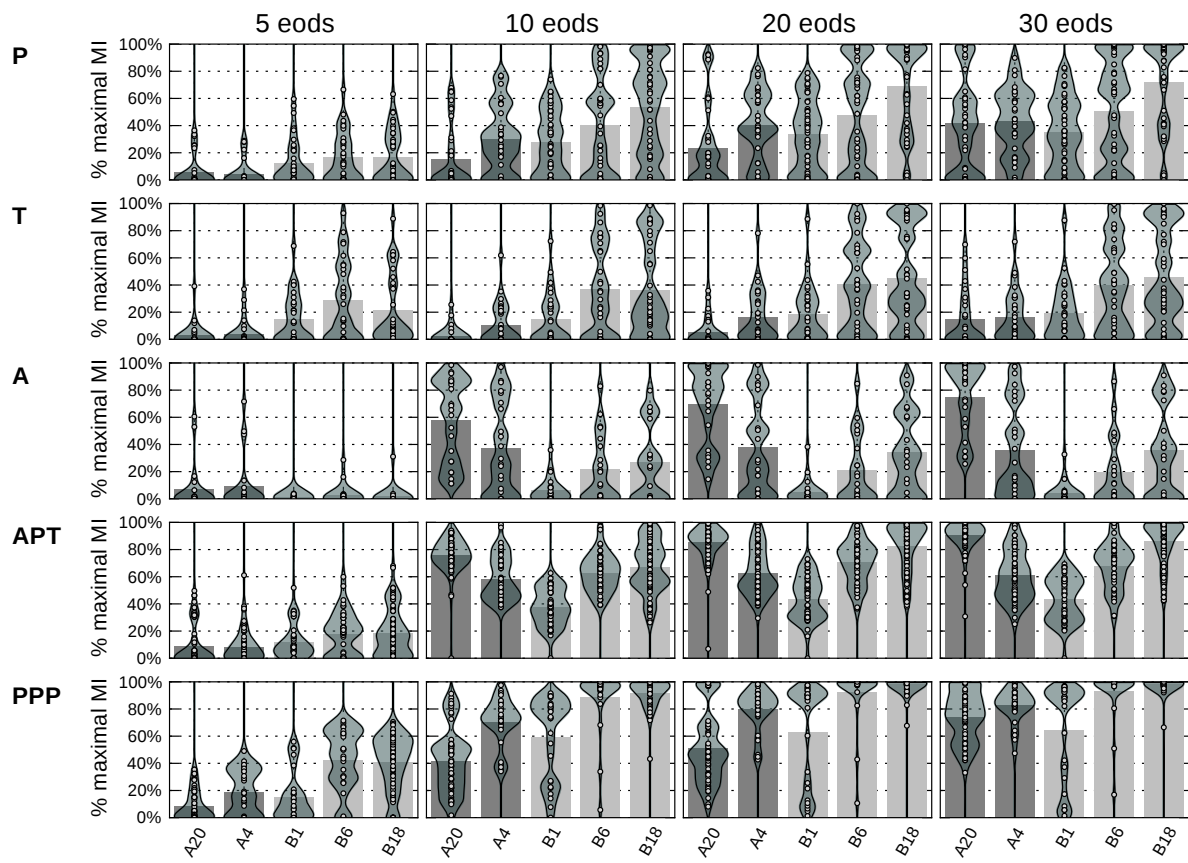


Figure 10

6 Legends

Figure 1: Characteristics of observed *Eigenmannia* chirps. **A-D** Top panels show voltage traces of electric organ discharges (EODs) containing chirps (light black lines) as well as the low-frequency component estimated by low-pass filtering of the EOD trace (bold black line, filter cutoff at 8 Hz). Bottom panels depict EOD frequency. Note that recordings originate from different animals and therefore EOD frequencies differ. **A** Single-cycle interruption. **B** Chirp consisting of several repetitions of single-cycle interruptions (type B chirp). **C** Interruption of more than one cycle length (type A chirp). **D** Chirp with complex frequency modulations. **E** Number of chirps emitted during 100 s stimulation and control. Significance was evaluated by paired-sample Wilcoxon signed-rank test ($n = 14$, $p = 0.0002$). **F** Distribution of chirp durations measured in EOD cycles averaged across animals ($n=14$). Error bars indicate standard deviation.

Figure2: Different chirp types generated distinct amplitude and low-frequency modulations. **A** Simulated interaction between receiving fish EOD (upper panel) and a chirp stimulus (middle panel), resulting in a regular sinusoidal amplitude modulation of the simulated fish EOD, the beat (black line). Chirps interrupted the beat and led to a sudden phase advance (compare black line and dashed gray line illustrating the time course of an uninterrupted beat). **B** Amplitude modulations (black lines) and low-frequency modulations (gray lines) resulting from stimulation with different stimuli. Each column contains a certain chirp stimulus (headings on top), each row illustrates the arising amplitude modulations perceived by the fish at different phase relations to the underlying beat. The first three columns show type B chirps. Column one shows a single-cycle interruption (B 1 chirp), columns two and three type B chirps of 6 and 18 EOD cycles duration (B 6 and B 18). Column four and five depict type A chirps of 4 and 20 cycles duration (A 4 and A 20). The low-frequency content of the stimuli was estimated by low-pass filtering (Butterworth low-pass filter, 15 Hz cutoff).

Figure 3: All three types of electroreceptors respond to the all chirp types. **A** The stimuli mimicked the EOD of a chirping fish (top row) that resulted in an amplitude modulation of the EOD of the receiving fish (stimuli were calibrated to modulate the EOD amplitude by 20%). **B** P-unit responses with spike rasters in the upper row, and peri-stimulus-time-histogram (PSTH) in the lower row, respectively. Shaded areas in the left panel mark the analysis windows. From left to right: *chirp response* (gray area, aligned with the chirp), *beat response* (dark gray area, same length and phase relation with the beat as the *chirp response*, but placed in an uninterrupted beat), and *control response* (gray area, covering a full beat cycle). **C** Responses and analysis windows of T-units (see B for details). Note that the lower row shows the inter spike intervals (ISI) relative to the average ISI recorded at rest instead of the firing rate. **D** Responses of ampullary receptors. Here, only the *chirp response* (grey) and *control response* (dark grey) were analysed.

Figure 4: Distinct response patterns to different chirp types in a 24 Hz beat in P-units.

Averaged responses of P-units to the different chirp types (see figure 2) in a 24 Hz beat. **A** Effects of chirps on the average firing rate, the response correlation, and the derivative of the PSTH were analysed for ten different phase relations between chirp and beat. **B** The firing rate was analysed for the onset (first EOD cycle) of the chirp. Error bars denote standard deviation. Measures in the *chirp response* (gray dots) and *beat response* (black dots) were normalized to the *control response* (horizontal line, compare figure 3). Asterisks indicate a $p < 0.01$ in a Wilcoxon signed-rank test between *chirp* and *beat response* (black asterisks) as well as *chirp* and *control response* (gray asterisks).

Figure 5: Similar P-unit response patterns to chirps in fast beats. Similar experiment and analysis as in figure 4, but chirps were now embedded in a 100 Hz beat.

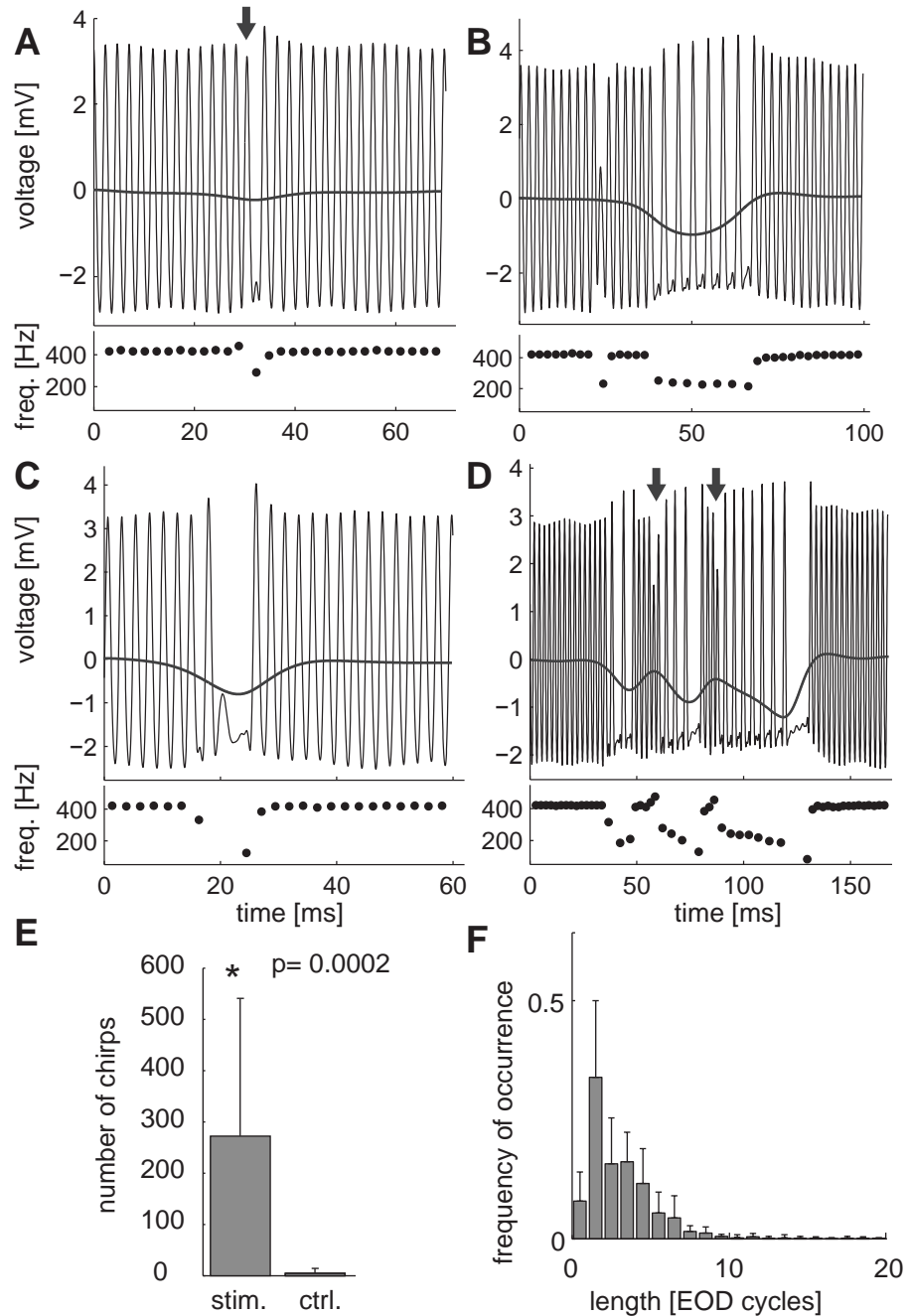
Figure 6: Response modulations of P-units with high and low baseline rate. A Time-courses of the AM received by the recorded fish for four chirp stimuli. **B** Responses of a P-unit with relatively low baseline firing rate (110 Hz, EOD rate 380 Hz). The upper panels show raster plot of 33 trials. Lower panel is the PSTH. **C** Same as **B** but of a P-unit with a high baseline firing rate (240 Hz, EOD rate 340 Hz).

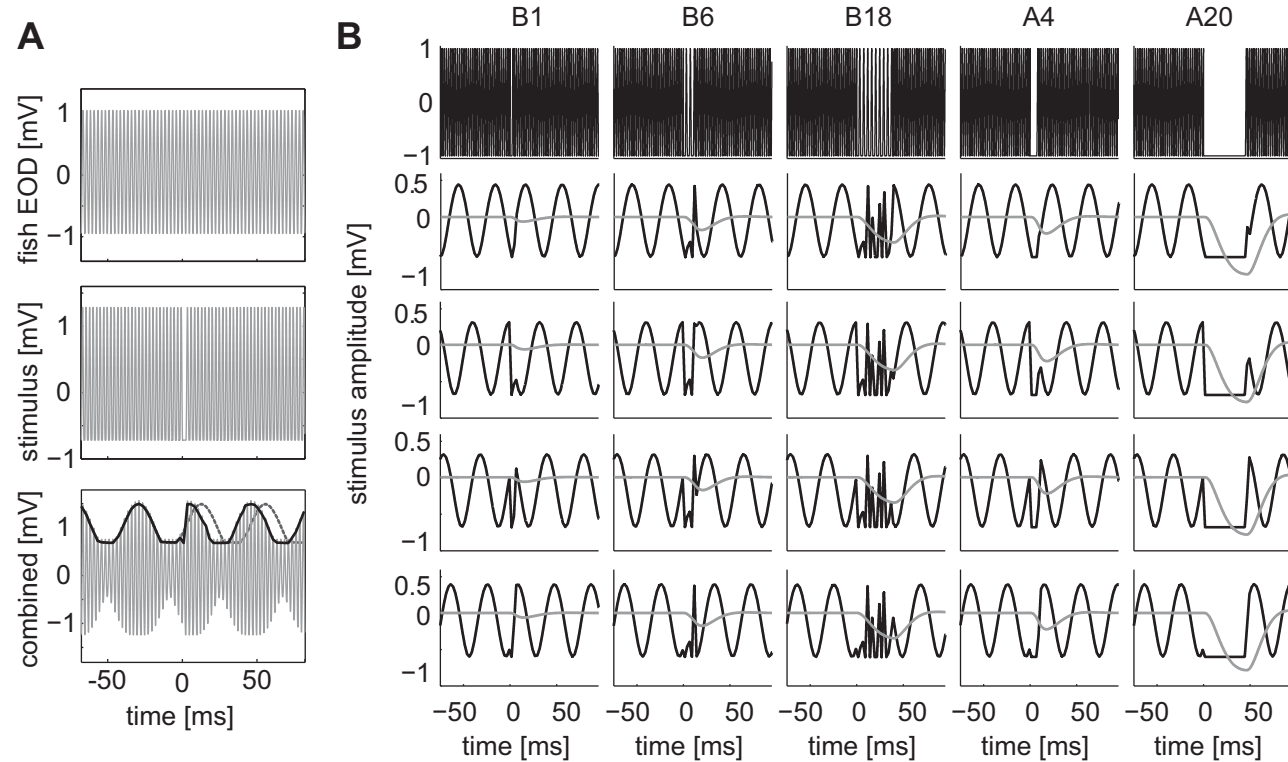
Figure 7: T-units respond to chirps with modulations in spike timing. Averaged responses of T-units to the different chirp types (compare figure 2) in a 24 Hz beat. **A** Effects of chirps on the inter spike interval (ISI, top row) and the ISI correlation between trials (bottom row) were analysed for ten phase relations between chirp and beat. **B** The ISIs were analysed for the onset (first EOD cycle) of the chirp. Error bars denote standard deviation. *Chirp response* (gray) and *beat response* (black) were normalized to the *control response* (horizontal line, compare to figure 3). Asterisks indicate a $p < 0.01$ in a Wilcoxon signed-rank test between *chirp* and *control response* (black asterisks) as well as *chirp* and *beat response* (gray asterisks).

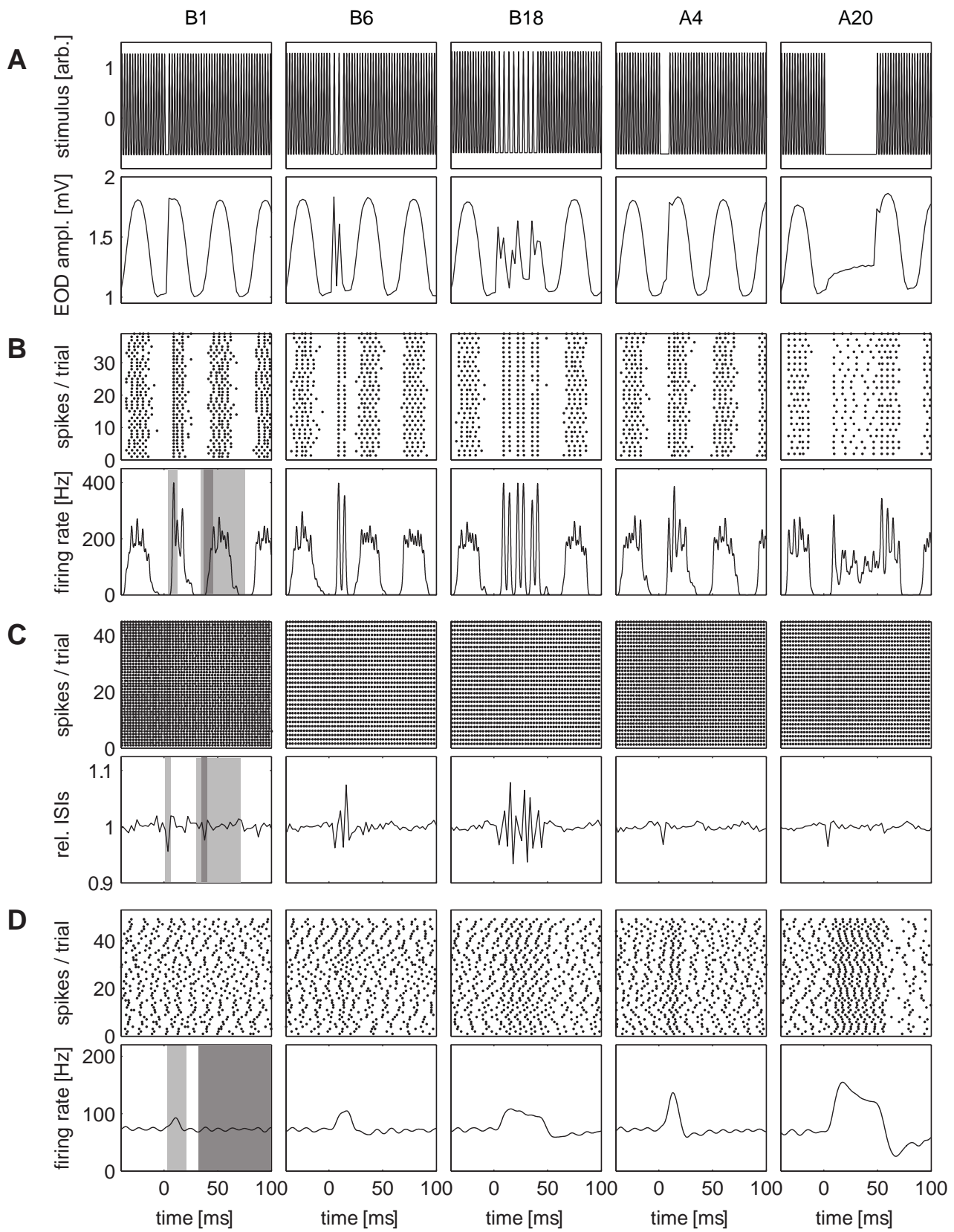
Figure 8: Quantitative analysis of ampullary responses to chirps. **A** The response duration and **B** response strength, as well as the mean derivative of the firing rate **C** and response correlation **D** of ampullary receptors were analysed and compared to the chirp duration and chirp strength (amplitude of the low-frequency component of the chirp, normalized to the value of B1 chirps at 20% contrast), respectively. Response strength, derivative of the firing rate and response correlation were normalized to the control firing rate, and the low-frequency component was normalized to the value of single-cycle interruptions. Dots show the mean, error bars the standard deviation. The slope (m) and the intercept (c) of the fit are indicated, as well as the correlation coefficient (r) and its statistical evaluation according to Pearson (p). Chirp types are indicated as abbreviations (compare figure 3).

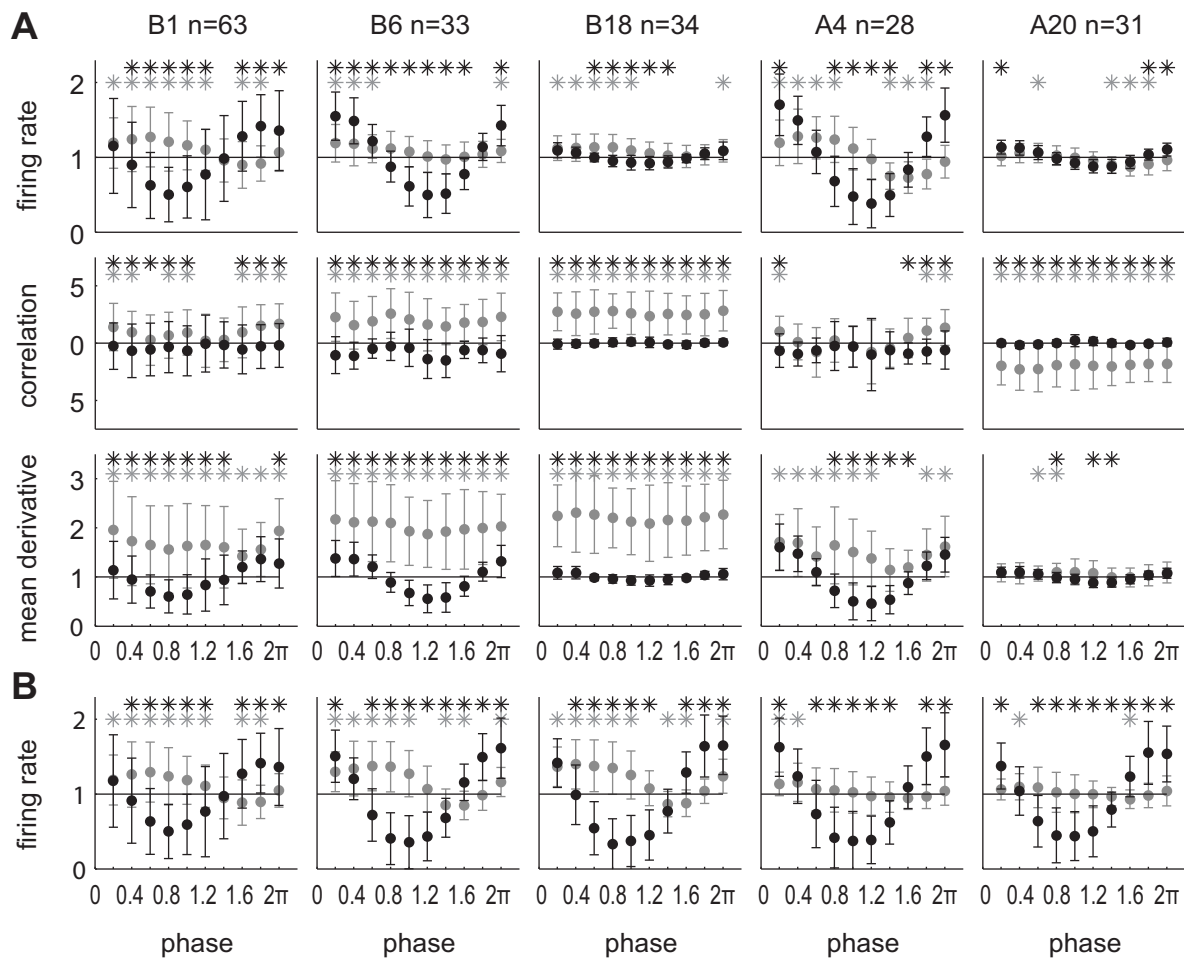
Figure 9: Decoding of a P-unit (A), a T-unit (B), and an ampullary (C) receptor response to certain chirps. Top panels show the stimulus, i.e. the electric field of the artificial second fish in arbitrary units. The label denotes the type of the chirp type B chirp of 18 cycles duration (B18) for the P- and T-unit and type A chirp of 20 EOD cycle duration (A20) for the ampullary receptor (note that the duration is given in relation to the chirping fish, not the receiving fish). The 2nd and 3rd panel illustrate the responses to the chirp (2nd panel) and a random selection to the beat alone (3rd panel) as spike rasters and PSTH estimated as the average across trials after convolution of spikes with a Gaussian kernel ($\sigma = 0.1$ ms). 4th panel illustrates the weighting function $w(t)$. It closely follows the difference between the baseline and the chirp PSTHs. For the responses of the P-unit and the T-unit upon a B18 chirp, the difference are most prominent after skipped EODs. For the response of the ampullary unit to a A20 chirp, the difference is strongest during the period of silence including some onset delay and a rebound response. 5th panel shows the decoding performance in percentage of the maximal mutual information (see methods). Decoding performance increases with increasing trial length.

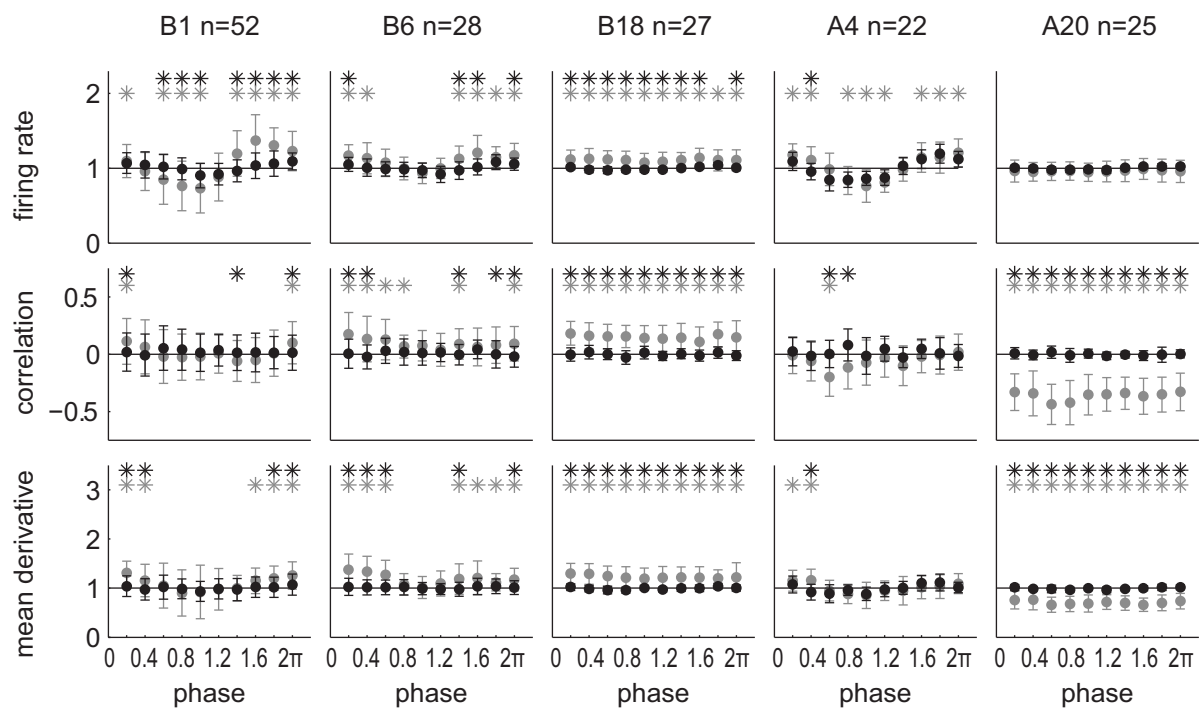
Figure 10: Decoding performance by cell/population vs. chirp type We report the decoding performance as mutual information between the actual label (chirp vs. baseline) and the predicted label normalized by the maximally achievable information. Letters denote the cell type or the cell types of each neuron participating in the population. Each single point denotes the average mutual information for one cell or population over ten training and test sets generated by resampling. The violin plots depict the smoothed histogram. The bars denote the mean. For all cell and population types, decoding performance increases with increasing length of the time window used for classification. P-units perform well on all chirp types, but better on B-type (first row). T-units also perform better on B-type chirps, but overall worse than P-unit and ampullary cells (second row). Ampullary units perform better on A-type chirps, in particular on the long A20 chirp (third row). Populations generally perform better than single units. For all chirp types except A20, populations of three P-units (PPP) perform significantly better than a population of an ampullary, a P-unit, and a T-unit. For A20 chirps, the situation is reverse ($p \leq 0.006$, two independent sample t-test, Bonferroni corrected for five comparisons).

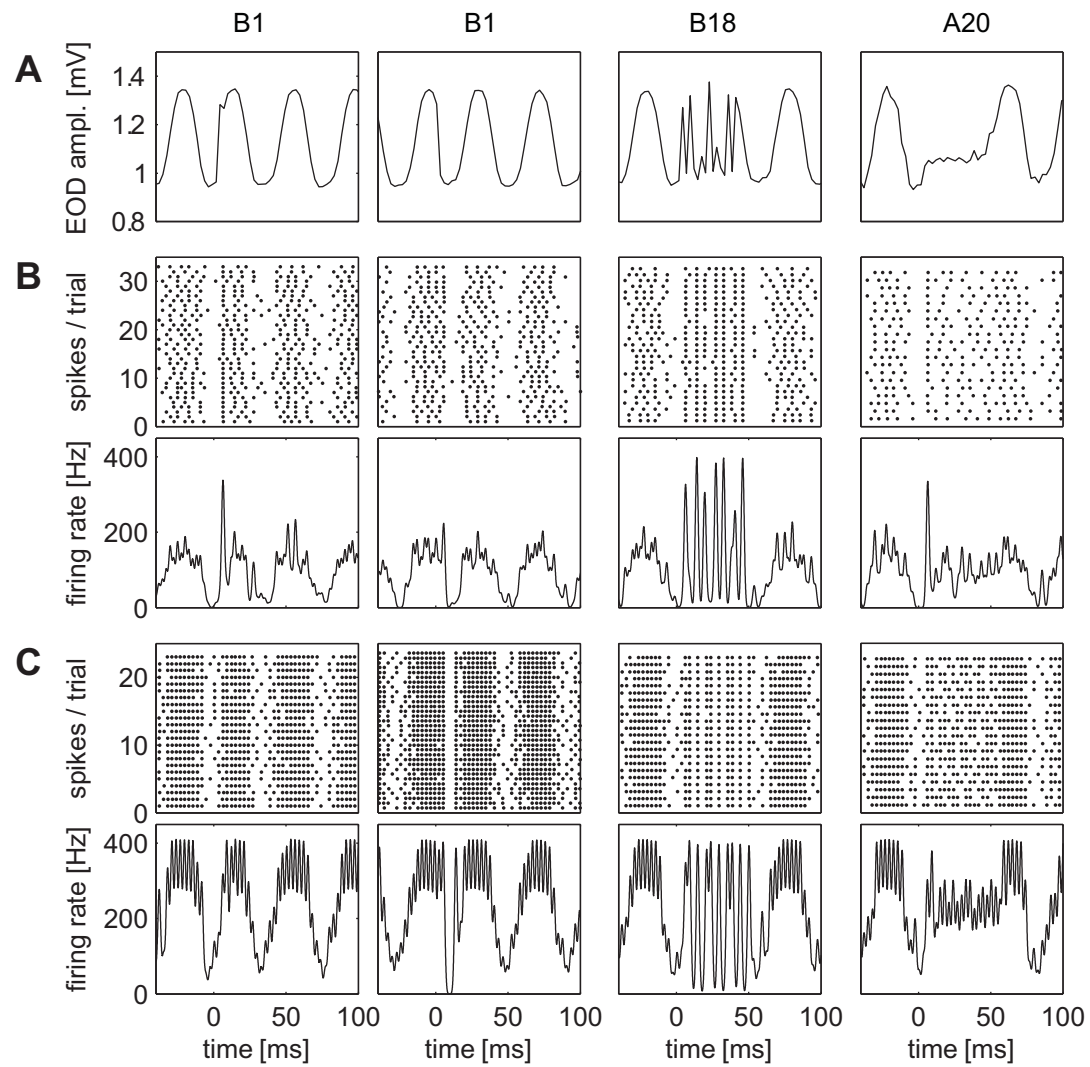


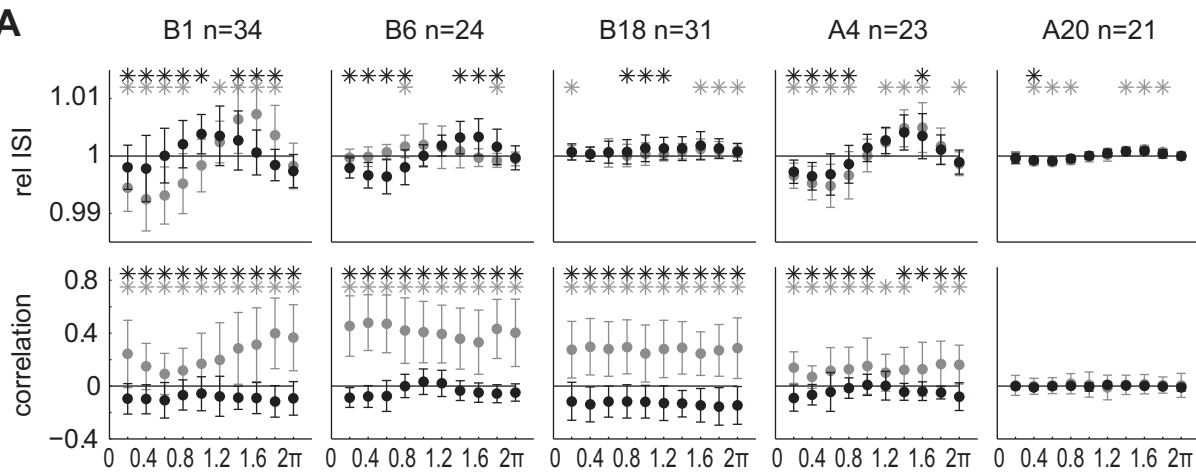










A**B**